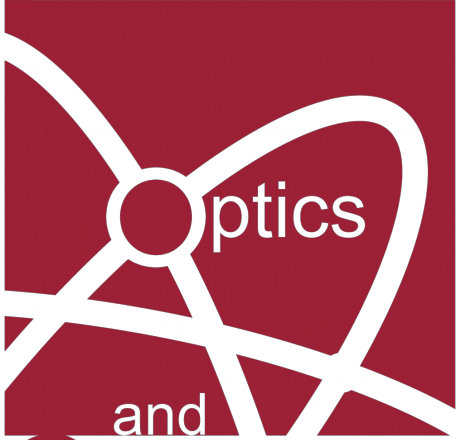# DEVELOPMENTS in

Optics

and

Communications

2018

Book of Abstracts

Riga, Latvia, April 12 – 13 , 2018

14th International Young Scientist conference

Developments in Optics and Communications 2018

Book of Abstracts

Cover design: Nellija Liepina

www.docriga.lv

Welcome

The Organizing Committee kindly welcomes you to the 14th International Young Scientist conference "Developments in Optics and Communications 2018". This conference is organized jointly by University of Latvia SPIE student chapter and OSA Latvian student chapter. The purpose of this conference is to bring together students and young scientists working experimentally and theoretically in the fields of optics and photonics to share and exchange new ideas and to establish contacts for future collaboration. The conference traditionally covers the following topics:

- Laser Physics and Spectroscopy;

- Biophotonics;

- Optical Materials and Phenomena;

- Optics in Communications;

- Vision Science.

The organizers wish you a fruitful conference and a pleasant and memorable stay in the capital of Latvia!

The Organizing Committee

DOC chairs

- **Emilija Vija Plorina**
  Bsc student, research assistant
  Riga Technical University

- **Artis Brasovs**
  PhD student

Organizers

- **Marta Lange**
  PhD student
  University of Latvia

- **Ilze Oshina**
  PhD student, researcher
  University of Latvia

- **Inga Brice**
  PhD student
  University of Latvia

- **Varis Karitans**
  Leading researcher
  Institute of Solid State Physics, University of Latvia

- **Brigita Zutere**
  University of Latvia

- **Arturs Cinins**
  Researcher
  University of Latvia

- **Lasma Asare**
  Dr.Phys.

- **Tatjana Pladere**
  PhD student

- **Matīss Lācis**
  Riga Technical University

- **Nellija Liepina**
  University of Latvia

Scientific committee

- **Prof. Ruvin Ferber**
  Faculty of Physics and Mathematics, University of Latvia

- **Prof. Maris Ozolins**
  Department of Optometry and Vision science, University of Latvia

- **Prof. Uldis Rogulis**
  Institute of Solid State Physics, University of Latvia

- **Prof. Janis Spigulis**
  Institute of Atomic Physics and Spectroscopy, University of Latvia

- **Prof. Jurgis Porins**
  Faculty of Electronics and Telecommunications, Riga Technical University

Program

VISION SCIENCE	OPTICAL MATERIALS AND PHENOMENA
BIOPHOTONICS	LASER PHYSICS AND SPECTROSCOPY

Thursday, 12th of April, Jelgavas street 1, The Academic Centre of University of Latvia	
8:30 – 9:00	Registration and coffee
9:00 – 9:30	Opening session
9:30 – 10:20	Vision Science: Invited speaker: **Linda Lundström** Visual Optics: Focus on the Periphery
10:20 – 11:10	Vision Science: Invited speaker: **Varis Karitans** Simulation of Vitreous Floaters using an Eye Model with Microfluidics System
	Student Talks: Vision science
11:15 – 11:30	**Sanita Liduma**: Changes in visual acuity, refraction and pachymetry in various stages of keratoconus after cross-linking operations
11:30 – 11:45	**Renars Truksa**: Development of realtime acquisition system for evaluation of potential melanopic dose and cone excitation in environmental light
11:45 – 12:00	**Zane Jansone**: Patient color vision sensitivity changes before and after cataract surgery
12:00 – 13:00	Lunch
13:00 – 13:50	Optical materials and phenomena: Invited speaker: **Edgars Nitiss** All-organic optical waveguide devices for communication and sensing applications
	Student Talks: Optical materials and phenomena
13:50 – 14:05	**Inga Jonane**: Structural investigations of thermochromic phase transition in copper molybdate
14:05 – 14:20	**Meldra Kemere**: Energy transfer in Dy3+/Eu3+ co-doped glasses and glass-ceramics containing fluoride nanocrystallites
14:20 – 14:35	**Andris Antuzevics**: Multisite formation in Gd3+ and Eu3+ doped SrF2 nanoparticles
14:35 – 14:50	**Julija Pervenecka**: Photoluminescence and Amplified Spontaneous Emission of Neat 4H-Pyran Derivative Containing Thin Films
14:50 – 15:00	Short break
15:00 – 16:30	Poster session (Vis + OptMat)
	Evening activities

Friday, 13th of April, Jelgavas street 1, The Academic Centre of University of Latvia	
9:00 – 9:50	Biophotonics: Invited speaker: **Igor Meglinski** Application of optical tweezers for examination of mutual interaction of red blood cells with nano-materials
	Student Talks: Biophotonics
9:50 – 10:05	**Marta Lange**: Non-invasive optical skin evaluation device for cancer screening
10:05 – 10:20	**Emilija Vija Plorina**: Method for skin disease classification using skin autofluorescence imaging
10:20 – 10:40	Coffee break
10:40– 11:30	Laser Physics and spectroscopy: Invited speaker: **Florian Gahbauer** Spin Detection using Nitrogen-Vacancy Centres in Diamond
	Student Talks: Laser Physics and Spectroscopy
11:30 – 11:45	**Arturs Bundulis**: Third-order nonlinear optical properties of thin organic films and solutions
11:45 – 12:00	**Darya Meniailava**: Theoretical insights into the electronic structure and low-lying states of the uranium nitride molecule
12:00 – 12:15	**Annija Lucija Fridmane:** Spectroscopic studies of bismuth containing electrodeless light sources working in self-modulating regime.
12:15 – 12:30	**Sandhra Mirella Valdma**: Single-shot fiber dispersion characterization with white light interferometry
12:30 – 12:45	**Reinis Lazda:** Measurement of ODMR signals from NV centers in diamond crystal, analysis of the signals
12:45 – 14:00	Lunch
14:00 – 15:30	Poster session (Bio+LasPhys)
	Closing Session
	Evening social event

Vision science: talks

Visual optics: Focus on the Periphery

Linda Lundström

KTH Royal Institute of Technology, Department of Applied Physics, Visual Optics Research Group

E-mail: linda.lundstrom@biox.kth.se

Vision is the most important sense for most people and a good optical correction, e.g. in the form of spectacles, is often taken for granted. However, it is relatively unknown how the optical errors in the peripheral visual field affect our vision. This presentation is about peripheral correction for myopia control and macular degeneration: how to measure and correct the wave front aberrations and what effects to expect.

SIMULATION OF VITREOUS FLOATERS USING AN EYE MODEL WITH MICROFLUIDICS SYSTEM

Varis Karitans

University of Latvia, Department of Optometry and Vision Sciences
E-mail: variskaritans@gmail.com

Vitreous floaters are one type of entoptic phenomena experienced by about 80 % of the entire population. They manifest themselves as bubbles, chains, cobwebs and other structures floating in the field of view. These are caused by cell bodies and protein structures floating in a liquified vitreous humour. Most often, they don't point to any pathological visual condition and simply cause visual discomfort. The only effective methods how to treat them are vitreolysis and vitrectomy. While effective, both these methods are associated with serious risks to the ocular health. That's why it is important to look for alternative solutions to this phenomenon.

Changes in visual acuity, refraction and pachymetry in various stages of keratoconus after cross-linking operations.

Sanita Liduma[1,*], Eva Vavzika[1], Gunta Krumina[1]

[1] *University of Latvia, Faculty of Physics and Mathematics, Department of optometry and Vision Science, Riga, Latvia*

E-mail: sanita.liduma@gmail.com,

Introduction: It is not possible to treat keratoconus but it is possible to stop its progression. If we diagnose keratoconus in time then we can make earlier cross-linking operation accordingly maintaining the corneal tissue in earlier keratoconus stage with better visual acuity. At present time collagen cross-linking operation with riboflavin and UVA is the best method to stop progressive keratoconus. Therefore cross-linking is the first choice for progressive keratoconus (Khattak, Nakhli & Cheema, 2015). Cross-linking operation stops keratoconus by stopping the formation of irregular astigmatism, reducing the rapid changes of corneal curvature, spherical equivalent and astigmatism for keratoconus patients (Coskuseven et al, 2009). In clinical practice, it has been seen that patients with lower keratoconus stage have better results after the operation, but till now there are no compelling studies which could prove that.

Method: In the study have been analyzed „Dr Lukin's eye clinic" cross-linking operations patients' records 6 months after the operation. Totally there have been analyzed 49 eyes with I, II and III keratoconus stage (patients age from 18 to 35 years). For patients, there have been determined best subjective refraction, uncorrected visual acuity and corneal thickness 6 months after the operation.

Results: I stage patients' visual acuity improved to 0.17 decimal values but to II and III stages patients had visual acuity 0.07 and 0.08. After the operation, there has been seen improvement in visual acuity during 6 months in all the keratoconus stages. Before operation the average spherical part of the eye refraction was -1.42±0.08 D and after 6 months the average spherical part reduced to -1.19±0.09 D, the astigmatism of eye refraction before operation was -2.90±0.07 D and after 6 months it increased to -3.26±0.07 D, the spherical equivalent before operation was -2.73±0,09 D and after 6 month – increased to -2.75±0.09 D. For all keratoconus stages (I, II and III) corneal thickness reduced to 7.56%, 6.54% and 9.27%, respectively.

Conclusion: Our study shows that the corneal collagen cross-linking operation is the effective procedure to stop keratoconus progression in all keratoconus stages thereby it is the first choice for progressive keratoconus. Our study also proves that if we set keratoconus to diagnose early than with cross-linking operation it is not only possible to stop but also improve visual acuity after the operation.

References

[1] Coskunseven, E., Jankov, MR. & Hafezi, F. Journal of Refractive Surgery, 25, 371-376 (2009).

[2] Khattak, A., Nakhli, F. & Cheema, H. Saudi Journal of Ophthalmology, 29, 249-254 (2015).

Development of realtime acquisition system for evaluation of potential melanopic dose and cone excitation in environmental light

Sergejs Fomins[1,*], Renars Truksa[2], Maris Ozolinsh[1], Gunta Krumina[2]

[1] *Institute of Solid State Physics, University of Latvia, Kengaraga 8, Riga, Latvia, LV-1063*

[2] *Optometry and Vision Science Department, University of Latvia, Jelgavas 1, Riga, Latvia, LV-1004*

*E-mail: sergejs.fomins@lu.lv,

Retinal ganglion cells contain circadian rhythm modulating pigment melanopsin. This pigment found in humans in 2000's is responsible for cascade of physiological events modulated by exposure to light [1]. There is effort to produce the autonomic systems for identification of melanopsin activating radiation in environmental light[2].

Previously, Kundrats etal (2016) presented our first system for measurement of melanopic light and simultaneous pupil tracking [3]. Besides the pupil tracking and static blue light sensor, the system had significant drawbacks. First, it is known that melanopsin sensitivity can be changed under different illumination condition. Second, pupil response has high correlation with photopic sensitivity. Third, the system was not optimal due to the computational efforts for pupil tracking. In our updated system two spectral sensitivities for blue light are applied to account for changing illumination conditions. Also the RGB sensors block is added for evaluation of potential light reaching the photopic system cones. The rationale for RGB sensors is the ability of system to discriminate between the artificial and natural illumination, as also to acquire the correlated colour temperature of the source. Acquired parameters are suitable for long-term ergonomic monitoring of corneal illumination and supplemental data in the study of physiological changes due to fatigue.
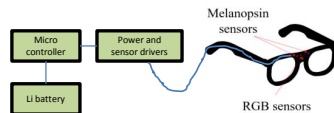

Figure 1: Sensor arrangement at the front brow-line of spectacles. Blue light sensors and colorimetric sensors are applicable.

References

[1] Lucas etal, Trends Neurosci **37(1)**, p.1-9 (2014)

[2] Miller etal, Lighting Res. Technol. **42**, p.271-284 (2010)

[3] Kundrats etal, DOC2016 Book of Abstracts, p.50 (2016)

Patient color vision sensitivity changes before and after cataract surgery

Zane Jansone[1], Maris Ozolinsh[2]

[1] *University of Latvia, Optometry and Vision science department, Riga, Latvia*
[2] *University of Latvia, Inst. of Solid State Physics, Riga, Latvia*

In optometrist practice we are dealing with patients who have cataract or have had cataract removal surgery. We check their vision functions but not their color vision. Color vision tests can give information about pathological changes in eye structures. Our aim was to evaluate if the color vision chromatic resolution changes before and after cataract surgery. We used saturated and unsaturated Farnsworth D15 Color vision arrangement test to check color sensitivity changes in confusion line directions. The results were analyzed in three ways: by summing the color differences between adjacent caps according to Bowman[1], by averaging color difference vectors according to Vingry and King -– Smith[2], and using linear regression line that is made from error cap arrangements[3]. In our research participated 26 eyes with cataract. Patients with glaucoma, macular diseases, diabetes, lower visual acuity than <0.10 decimal units, were excluded from research.
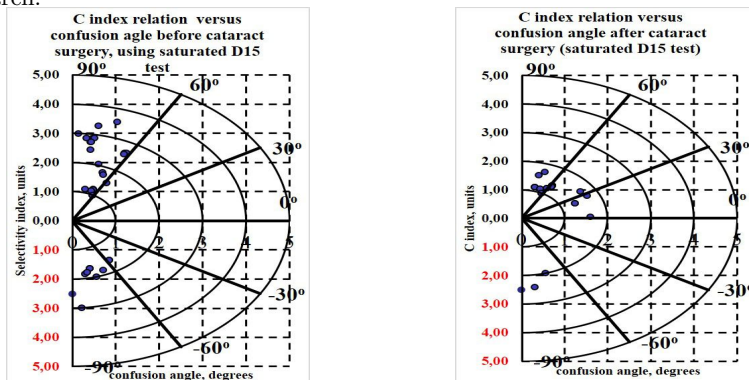

Figure 1: C index relation versus confusion angle before and after cataract surgery.

All three tests showed that cataract caused lens opacities to decrease significantly in visible light chromatic resolution. Before the cataract surgery, the D15 test stimulus arrangement sequence showed similarities with tritan color deficiency. Two patients showed improvements in color vision sensitivity, but they still had deviations from the norms, meaning that the color vision sensitivity changes not only due to the lenses' light absorption but from other pathological factors as well.

References

[1] Bowman, K. J. ,A Method for Quantitative Scoring of The Farnsworth Panel D-15, Acta Ophthalmologica **60(6)**, 907 - 916 (1982)
[2] Vingrys, A.J., Quantitative Scoring Methods for D15 Panel Tests in the Diagnosis of Congenital Color Vision Deficiencies, Optometry and Vision Science **68(1)**, 41 - 48, (1991)
[3] Foutch, B. K., Stringham, J. M., & Lakshminarayanan, V.,A new quantitative technique for grading Farnsworth D-15 color panel tests, Journal of Modern Optics **58(19)**, 1755 - 1763 (2011)

Vision science: posters

Peripheral illusory movement time dependencies

Justine Aispure,[1] Olga Danilenko,[1] and Maris Ozolinsh[1,2]

[1] *Dept.of Optometry and Vision science, Univ.of Latvia, Jelgavas 1, Riga 1003, Latvia*
[2] *Inst. of Solid State Physics, Univ.of Latvia, Jelgavas 1, Riga 1003, Latvia*
* E-mail: ozoma@latnet.lv

Illusion *Break of the curveball* [1] was firstly demonstrated in the Illusion Contest where it was awarded as the best illusion of the year (Shapiro, http://illusionoftheyear.com/2009/05/the-break-of-the-curveball/). Authors explained essence and some details of perception mismatch in another paper [2]. They have shown that visual perception of the trajectory of a falling ball deviates from vertical if the ball is spinning and contains texture and direction of the sight of view is peripheral. We studied the phenomenon comparing slants of two falling balls viewed in opposite peripheral areas: reference object a) uniform and neutrally gray falling at distinct angle; and b)textured object: falling vertically, with vertical stripe structure that moved along horizontal direction within the object area. 2AFC paradigm: is the reference object slope steeper; was used to build psychometric curves.
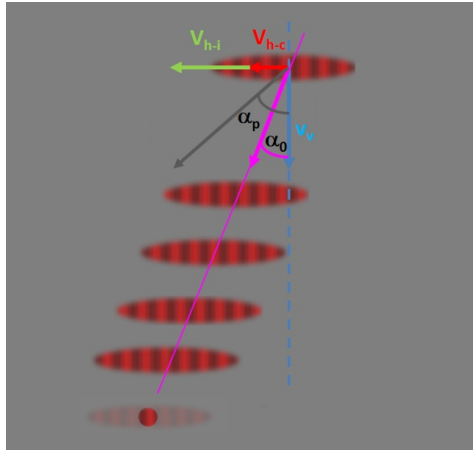

Figure 1: Break of curveball illusion. Observer perceives a vertically falling ball (in Part I; in Part II at slope ALFAo) in eye periphery as an oblique motion (overestimation of the slope by ALFAp)) if the ball is spinning. Observers task is to decide: is the slope of the illusory motion in the left periphery steeper as a real slope at the right periphery (no spinning here). Modulated grating translates (Vh-i) to right.

Observers in Part I were nave participants that during one hour responded to series of events where reference objects had randomly selected slant of fall trajectory. Subjective equivalence point was determined at centres of sigmoidal fit of psychometric curves where ordinate was a reference real slant. Averaged (22 participants) illusionary slant of falling textured objects between was ALFA = 28 +/-5deg (for viewing directionality 8deg; falling vertical speed 0.18deg/sec, texture Michelson-contrast 0.82, spinning speed

Local information analysis in biological motion perception

Ilze Ceple[1,*], Jurgis Skilters[2], Vsevolod Liakhovetckii[3], Inga Jurcinska[1], Gunta Krumina[1]

[1] *Department of Optometry and vision science, Faculty of Physics and mathematics, University of Latvia, Rainis blvd. 19, Riga, Latvia, LV-1586*

[2] *Laboratory for Perceptual and Cognitive Systems, Faculty of Computing, University of Latvia, Rainis blvd. 19, Riga, Latvia, LV-1586*

[3] *Pavlov Institute of Physiology, Russian Academy of Sciences, St.Petersburg, Russian Federation*

[*] *E-mail:* ilze.ceple@lu.lv,

In 1973 Swedish psychophysicist Gunnar Johansson demonstrated that in human motion perception it is sufficient to demonstrate only the motion of the major joints in order to perceive a clear impression of a human shape, actions and characteristics. Since then there have been many debates whether biological motion perception is based on single point motion analysis (local information) or based on global perception of the whole object (Poljac et al., 2011; Cutting et al., 1988). The current study analyzes the attentional processes in biological motion perception and explores the significance of local information in determining between a point light walker and its scrambled version.

The results of 5 participants demonstrate that average reaction time for determining between biological motion and its scrambled version is 632 ms when the object is a biological motion stimulus and 719 ms when the scrambled version is demonstrated. These results agree with Sternberg (1969), as well as with Lappe et al. (2015) indicating that biological motion perception is based on specific sensory information filters. These filters analyze specific posture information and therefore can facilitate information analysis processes.

Eye tracking was applied as an objective method for analyzing the processes of direct and indirect attention. The average gaze duration on different biological motion areas (chest, hips or legs) demonstrate which parts of body attract direct attention more and are the most informative in biological motion detection. Eye tracking results demonstrate that when the task is to discriminate between biological motion and its scrambled version the average gaze duration in longer on the upper part of the body (67 percent) and the hips (29 percent). The information of feet motion in this case is less important that when discriminating motion direction.

References

[1] Cutting, Moore, Morrison, Perception and Psychophysics **44(4)**, 339-347 (1988)

[2] Poljac, Vervaillie, Wagemans, Perception **40**, 87 (2011)

[3] Sternberg, American Scientist **57(4)**, 421-457 (1969)

[4] Lappe, Wittinghofer, Lussanet, Frontiers in Integrative Neuroscience **9**, 24 (2015)

Effects of envioremental factors on tear osmolarity.

K. Dumberga[1], E. Kasaliete[1], A. Petrova[1], G. Krumina[1]

[1] *University of Latvia, Faculty of Physics and mathematics, Department of Optometry and Vision Science, Jelgavas street 1, Riga, Latvia, LV-1004*

Efficient tear production and turnover is essential to protect ocular surface. Elevated tear osmolarity is a key factor in the chain of events leading to dry eye disease (DED). Tear hyperosmolarity results from reduced tear flow and- or increased evaporation of aqueous tear phase, that leads to tear film breakup. Tear hyperosmolarity causes cell apoptosis of both cornea and conjunctiva, and secondary inflammatory events leads to further cell death and loss of goblet cells, that in turn promotes tear film instability. Tear film instability and hyperosmolarity are part of chronic neurogenic inflammatory process, that aggravates severity of DED (Potvin, 2015.).

Tear osmolarity is influenced by many inner and external factors. There is positive correlation between hydration level of whole body, expressed as plasma osmolarity, and tear film osmolarity (Bron, 2017.). Both are elevated in patients with DED. Quality and thickness of tear film lipid layer affects evaporation rates from tear film (Arciniega, 2011.). When quality or integrity of lipid layer is insufficient, evaporation loss and tear film osmolarity will increase (Yokoi, 2008.). As could be expected, evaporation loses are related to tear film surface area (Tsubota, 1995). Such inner factor as blinking rate affects tear osmolarity. It could be expected that, when blinking interval increases tear osmolarity grows also (Ousler 3rd, 2008.). External factors that changes tear osmolarity are temperature, humidity and air flow. The impact of environmental factors on each person is different, depending on individual adaptation (Potvin, 2015.). Exposure to low humidity for short periods as 90 min. causes frequent blinking, local discomfort and elevated levels of cytokines and proteases in aqueous tears (Alex, 2013).

Quantitative measure of osmolarity is number of osmoles of solute per litre of solution(mOsm/L). Dry Eye Workshop DEWS II (2017) proposes classification of tear osmolarity levels- normal - 302 +/- 8 mOsm/L, mild to moderate hyperosmolarity - 315 +/- 10 mOsm/L, severe form of DED - 336 +/- 12 mOsm/L (Sullivan, 2010.).

References

Alex A., Edwards A., Hays J.D., Kerkstra M., Shih A.& de Paiva C.S., Investigative Ophthalmology and Visual Science **54**, 11312-1132 (2013)

Arciniega J.C., Wojtowicz J.C., Mohamed E.M. & McCulley J.P., Cornea **30**, 843-847 (2011)

Bron A.J., dePaiva C.S., Chauhan S.K., Bonini S., Gabison E. E., Jain S., Knop E., Markoulli M., Ogawa Y., Perez V., Uchino Y., Yokoi N., Zoukhri D.& Sullivan D., The Ocular Surface **15**, 438- 510 (2011)

Yokoi N.,Yamada H., Mizukusa Y., Bron A.J., Tiffany J.M., Kato T.& Kinoshita S, Investigative Ophthalmology and Visual Science **49**, 5319-5324 (2008)

Ousler 3rd G.W., Hagberg K.W., Schindelar M., Welch D.& Abelson M.B., Cornea **27**, 509-513 (2008)

Potvin R., Makari S., & Rapuano C. J., Clinical Ophthalmology **9**, 20392047 (2015)

Tsubota K., Nakamori K., Archives of ophthalmology **113(2)**, 155-158 (1995)

Effects of environmental factors on anterior eye structures

Linda Eglite, Evita Kassaliete, Anete Petrova, Gunta Krumina

University of Latvia, Faculty of Physics and Mathematics, Optometry and Visual Science Department, Riga, Latvia

*E-mail: lindish211@inbox.lv,

Office workers spend most of their work time on a computer. At intense work, many of these employees experience a computer vision syndrome - a combination of multiple vision problems (diplopia, blurred vision, headache, eye discomfort, dryness, photophobia, burning) (Tauste et al., 2015; Tilborg et al., 2017). Computer users may have several eye-related problems, such as reduced tear stability, incomplete blinking, reduced blinking. In order to improve the well-being of office staff, it is necessary to improve office layout, lighting, air quality. here are several factors that determine the air quality of the office: low relative humidity, high air temperature, high air pollution, high air ventilation. 29.9 percent of office workers have seen moderate or severe complaints of visual discomfort and dryness (Portello et al 2012). People complaints who have reduced tear film can be caused by various factors: environmental factors (low air humidity and high air temperature, air pollution, air humidity), a task that requires increased attention (while focusing the blinking of the eye decreases from 16,8 times per min to 6,6 times per minute (Schlote et al., 2003), as well as concentrating the eyes open more widely and discovering a larger part of the surface of the eye that promotes the dehydration of the tear film), individual factors such as the use of contact lenses, meibomian gland dysfunction , tear film stability and other factors. In Kluizenaar et al. (2016) research has found that 34 percent of 7441 office workers complained about various eye problems associated with dry eye syndrome. However, most of those participants (91.2 percent) who had complaints did not felt these sypmptoms or had reduction of symptoms when they were outside the office.

References

[1] Kluizenaar, Y., Roda, C., Dijkstra, N. E., Fossati, S., Mandin, C., Mihucz, V. G., Hanninen, O., de Oliveira Fernandes, E., Silva, G. V., Carrer, P., Bartzis, J. Bluyssen, P. M. Building and Environment **102** 54-63 (2016)

[2] Portello, J. K., Rosenfield, M., Bababekova, Y., Estrada, J. M. Leon, A. Ophthalmic and Physiological Optics **32:5**, 375-382 (2012)

[3] Schlote, T., Kadner, G., Freudenthaler, N. Graefes Arch Clin Exp Ophthalmol **242** 306-312 (2003)

[4] Tauste, A., Ronda, E., Molina, M. J., Segui, M. Ophthalmic and Physiological Optics **36** 112119 (2016)

[5] Tilborg, M. M., Murphy, P. J., Evans, K. S. Optometry and Vision Science **94** No. 6, PP. 688-693 (2017)

Development of global stereotest for stereoanomaly

Elizabete Eldmane[1,*], Vsevolod Lyakhovetskii[2], Gunta Krumina[1]

[1] *University of Latvia, Faculty of Physics and Mathematics, Department of Optometry and Vision Science, Riga, Latvia*

[2] *Pavlov Institute of Physiology, Russian Academy of Sciences, Saint-Petersburg, Russia*

[*] *E-mail:* elizabete.eldmane@gmail.com,

Stereotest can consist of three kinds of disparity zero, crossed and uncrossed disparity. Stereoanomaly is a condition where the subject cant distinguish one or two of three disparities types. For example, the crossed disparity is normal, while uncrossed disparity is changed and *vice versa. Richards* (1970) was one of the first who researched stereoanomaly, concluding that 30% of people have stereoanomaly using local stereotest with display duration 80ms. After his work many researchers continued studies to find out the prevalence of stereoanomaly in general population. *Jones* (1977) using local stereotest tested vergence eye movements for stereoanomalous individuals concluding that incorrect vergence eye movements is associated with stereoanomaly, using convergence when divergence is needed and *vice versa*. There are different kinds of global stereotests used in research. In the clinic, the most popular test is TNO stereotest. In research, most used global stereotests are anaglyph random dot stereogram or dynamic random dot stereogram using polarized or red-green glasses. There is still no research that has proven if stereoanomaly also occurs testing fine disparity.

Purpose of our study was to develop the new global stereotest and to evaluate how many stereoanomalous subjects are in our population using this new global stereotest with the possibility to change the time limit and the disparity size.

In our study, the global stereotest consists of the red and green random dots and there are no monocular cues for stereoblind subjects. The test generates the stimuli with different disparities and we use the staircase method principle for the evaluation of stereothreshold. Stimuli duration were with the restricted and with the unlimited presentation time. We compared our results with the standard TNO stereotest performed at 40cm using red-green glasses. In our pilot study, the first results have revealed that using display time less than 200ms subjects struggle to see stimuli. *Stelmach & Tam* (1996) using dynamic global random dot stereotest concluded that stereoanomaly is strongly affected by display time and test methods, some individuals need more time with crossed than uncrossed disparity and *vice versa*.

In conclusion, taking in consideration resent pilot study - display duration time will change and subjects stereoacuity will be measured depending on time.

References

Jones, R. (1977). Anomalies of disparity detection in the human visual system. *The Journal of Physiology*, 264(3), 621-640.

Richards, W. (1970). Stereopsis and stereoblindness. *Experimental Brain Research*, 10(4), 380-388.

Stelmach, L.B., & Tam, W.J. (1996). Stereo-anomalous vision in a sample of young adults. *SPIE Human Vision and Electronic Imaging*, 2657, 302-306.

Development of local stereotest for stereoanomaly

Annija Gulbe[1*], Vsevolod Lyakhovetskii [2], Gunta Krumina[1]

[1] *University of Latvia, Faculty of Physics and Mathematics, Department of Optometry and Vision Science, Riga, Latvia*

[2] *Pavlov Institute of Physiology, Russian Academy of Sciences, Saint-Petersburg, Russia*

[*] *E-mail:* annija.gulbe@gmail.com,

Introduction

Stereoanomaly is claimed to be a disability to distinguish whether the object is crossed or uncrossed disparity in depth perception. It has been reported that approximately 30% of the population fails to detect the object orientation in depth making a false judgment on perceived object being closer (crossed disparity) or further (uncrossed disparity) in the 3-dimensional test (Richards, 1971). Since then many factors have been considered and argued that limited duration of stimulus affects the presence of stereoanomaly (van Ee & Richards, 2002). Our goal is to make a new local stereotest to evaluate whether the limited duration of demonstrated stimulus affects the performance of crossed and uncrossed disparity perception in depth.

Method

The new stereotest was based on local stereopsis, designed as red-green anaglyph computer program, and was demonstrated separately to both eyes with red-green filters. The distance from test and subject was fixed and stimulus duration was limited. The subject was introduced with the task before any data recording. The test measured the crossed and uncrossed stereopsis threshold in small disparity using improved the staircase method. We expect to detect stereoanomaly prevalence in young adults and we believe that limited duration of demonstrated stimulus will distinguish symptomatic (stereoanomalous) from normal subjects using small disparity local stereopsis. Our pilot study presented that the duration of demonstrated stimulus impact stereoacuity threshold and presence of stereoanomaly, therefore it is crucial to be able to detect the duration of given answers. In clinical findings, the standard crossed stereotests are possible to use for uncrossed disparity by rotating the test in 180 degrees, but this test is without the limitation of time. Here we suggest a new method for the evaluation of crossed and uncrossed disparity and presence of stereoanomaly.

Conclusion

The main idea of the study is to design a new kind of local stereotest to evaluate clinically the presence of stereoanomaly and detect any difference in performance of crossed and uncrossed disparity in depth perception.

References

Richards, W. (1971). Anomalous stereoscopic depth perception. *Journal of the optical society of America*, 61(3), 410-414.

van Ee, R., Richards, W. (2002). A planar and a volumetric test for stereoanomaly. *Perception*, 31 (1), 51-64

Accuracy of visual depth perception depending on spatial layout of stimuli on volumetric display

Vita Konosonoka*, Tatjana Pladere, Karola Panke, Gunta Krumina

Department of Optometry and Vision Science, Faculty of Physics and Mathematics, University of Latvia, Jelgavas 1, Riga, Latvia, LV-1004
*E-mail: vita.konosonoka@gmail.com

Radiologists look through large amount of stacked images obtained in computed tomography to evaluate anatomical abnormalities that requires excellent depth estimation skills [1]. The performance quality depends on the cognitive load which increases due to a lack of the third dimension in the images, as well as different distractions that professionals experience at everyday work [1, 2]. It is suggested that the depth estimation performance can be positively influenced by using a volumetric display which produces images in a true physical depth. But the expected advantages of an innovative representation should be supported by the appropriate reaction of the visual system on its stimuli. Therefore, the purpose of our study is to investigate the interference of stimuli location and human factors on the accuracy of depth estimation on a multi-planar display.

Nine individuals aged from 21 to 29 years took part in the study. In each trial, the visual stimuli (four circles) were presented on a volumetric display consisting of 20 planes. The task was to distinguish which one was located closer comparing to the reference circles. The viewing time was unlimited but participants were instructed to complete the task quickly and precisely, as well as evaluate the perceived difficulty afterwards. The stimuli were located at one of three eccentricities ($1.9°$, $3.8°$, $7.6°$) and in one of four depth segments (1st-5th, 6th-10th, 11th-15th, 16-20th display plane).

The accuracy of perceiving relative depth differences at $1.9°$ and $3.8°$ eccentricities was highly precise in all four depth segments when the response time was less than 1250 ms or more than 2000 ms. Nevertheless, the average response accuracy slumped at $7.6°$ stimuli eccentricity that could happen due to limitations of visual acuity in the periphery, consequently leading to a higher cognitive load. The subjective evaluation of task difficulty matched moderately the response accuracy of participants. On the whole, our study has shown that the accuracy of depth estimation is more influenced by two-dimensional layout of visual stimuli rather than their location in depth of a volumetric display which is also reflected in the subjective evaluation of perceived task difficulty.

References

[1] Williams, L. H., Drew, T. Distraction in diagnostic radiology: How is search through volumetric medical images affected by interruptions? *Cognitive Research: Principles and Implications*, 2(1):12 (2017)

[2] Konstantinou, N., Beal, E., King, J.-R., Lavie, N. Working memory load and distraction: dissociable effects of visual maintenance and cognitive control, *Attention, Perception and Psychophysics*, 76:1985-1997 (2014)

The effect of blinking quality and quantity on tear film stability

Inese Loca*, Evita Kassaliete, Anete Petrova, Gunta Krumina

*Department of Optometry and Vision Science, Faculty of Physics and Mathematics,
University of Latvia, Jelgavas str. 1, Riga, Latvia, LV-1004*

E-mail: inese.loca@fizmati.lv

Dry eye disease is multifactorial illness of anterior eye structures. In research done by Hashemi et al. (2014) it was determined that about 8.7 % out of 1008 patients had it. One of the causes of dry eye is incomplete blinking when patients work on a computer. Their blinking is incomplete eyelids do not make complete contact therefore complete tear film cannot form on the cornea (Friedman, 2010). In study done by Portello et al. (2012) it was concluded that office workers spend on average 6 hours per day looking at the computer screen which directly correlates dry eye disease symptoms. Also it was determined that women suffer from this illness more than men.

The quality and quantity of blinking determines the stability of tear film. Hirota et al. (2013) did a study on 11 participants which concluded that working on a computer doing tasks that require high amounts of concentration reduces amount of times the participants blinks. Tear film destabilized with each incomplete blink. A study was conducted by Cardona et al. (2011) which tested participants age 21-28 that did not have any complaints regarding dry eye disease. Participants had to play computer games by looking at the screen at an angle. Afterwards the tear film stability and the high of tear meniscus was measured. It was concluded that frequency of the blinks decreased and amplitude of the blinks changed. The amount of incomplete blinks also increased. After this experiment stability of the tear film had decreased. Both studies concluded that high concentration tasks with computer correlates with destabilization of tear film. The position of the computer screen also affects the stability of tear film. The aim of this research is to find out how blinking quality and frequency reduces the stability of the tear film, and if the interior or the office somehow affects it as well.

References

[1] Cardona, G., Garca, C., Sers, C., Vilaseca, M., Gispets, J, Current Eye Research **36(3)**, 190-197 (2011)

[2] Friedman, N. J. Current Opinion in Ophthalmology, **21(4)**, 310-316 (2010)

[3] Hashemi, H., Khabazkhoob, M., Kheirkhah, A., Emamian, M. H., Mehravaran, S., Shariati, M., Fotouhi, A. Clinical and Experimental Ophthalmology, **42(3)**, 242-248 (2014)

[4] Hirota, M., Uozato, H., Kawamorita, T., Shibata, Y., Yamamoto, S. Optometry and vision science, **90(7)**, 650-657 (2013)

[5] NPortello, J. K., Rosenfield, M., Bababekova, Y., Estrada, J. M., Leon, A. Ophthalmic and Physiological Optics **32(5)**, 375-382 (2012)

Refraction changes: are daily technologies use responsible?

Kristine Mackare[1,*], Anita Jansone[1]

[1] *Faculty of Science and Engineering, University of Liepaja, Kr.Valdemara Str.4, Liepaja, Latvia, LV-3401*

*E-mail: kristine.mackare@gmail.com

Based on large-scale studies, by the year 2000 more than 22% of the world population had been diagnosed myopia, but more recent data shown that by 2015 - more than 30%. As the trend continues, it is expected that by the year 2050, at least half of the world's population will be myopic. The size of the myopia is also increasing and the age at which the myopia starts, continuing to development and progress. [1, 2]

Responsiveness for the progression of myopia is the high near work load and its impact on vision that is occurring today daily, especially by development of technology. All near work, especially small works, and crafts, viewing texts and images, reading, learning both print media and computer screen, playing games, etc., are considered to be near works.

Have been analysed 306 data of authors patients in 2017: age, gender, is the vision test first-time or repeated, does they have discomfort symptoms of vision, are glasses prescribed, is the progress in refraction, is the changes in vision found, do they use a computer.

Result shown, at least 91% of optic patients are using a computer, in addition, patients to the age of presbyopia - 99%. Almost 30% of computer users under the age of 40 performed a first-time vision test, because they have complaints of vision or various discomfort symptoms that arose when they are working at a computer. Everyone had a vision check and deviations from the norm in the visual state have been found that confirmed the complaints. Also, for those computer users who performed repetitive tests, changes in vision correction, as compared to existing glasses, were detected. For computer users under 40 years of age, an average change of 0.45D was detected within 1-2 years. Also, in all patients over the age of 40, changes in vision refraction were noted, but they may be due to the fact that patients have presbyopia, where the change is based mainly on lens elasticity changes and other pathological changes in eye structures.

References

[1] Holden B.A., Fricke T.R., Wilson D.A., Jong M., Naidoo K.S., Sankaridurg P., Wong T.Y., Naduvilath T., Resnikoff S., Global Prevalence of Myopia and High Myopia and Temporal Trends from 2000 through 2050 AAO Journal **Volume 123, Issue 5**, p 1036 - 1042 (2016)

[2] Professor Naidoo K., Myopia: A Growing Clinical and Public Health Challenge of Our Time presentation at 100% optical

The effect of distance on inattentional blindness

Sabine Matulevica[1*], Jurgis Skilters[2], Gunta Krumina[1]

University of Latvia

[1]*Faculty of Physics and Mathematics, Department of Optometry and Vision Science*
[2]*Faculty of Computing, Laboratory for Perceptual and Cognitive Systems*

Riga, Latvia

E-mail: sabinematulevica@gmail.com,

Introduction

To detect something, just looking at it is not enough. Inattentional blindness is a cognitive phenomenon when people fail to notice a completely visible, but unexpected object while attention is engaged in another object, task or event (*Simons*, 2000). Our research aim is to determine how the distance and accordingly the angular size of the stimulus on the retina affects the results of inattentional blindness task.

Method

139 women and 55 men (age 18-60 years) participated in our study. They were seated in different rows from the projection screen, which allowed us to get different distances and object angular sizes on the retina. Two inattentional blindness videos were shown and a primary task was given. At the end of each video, observers were asked a series of questions to determine whether or not they saw the unexpected object and how precisely the primary task was done. The angular size of the video and the unexpected object was calculated for each distance.

Results

Of all participants, only 1% responded correctly to all question an unexpected object in the first video "Invisible gorilla" (*Simons & Chabris*, 1999) and 6% of participants in the second one "Candy eating" (*Frischer et.al.*, 2011). Regardless of the distance and the angular size of the object, the number of participants (%) with the inattentional blindness was similar

Conclusion

The relationship between the presence of inattentional blindness and the angular size of the object is not obtained. Observers with inattentional blindness do not complete the primary task more precisely than the observers who spot the unexpected object. Level of inattentional blindness is higher in the first video ("invisible gorilla").

References

Simons, D.J. (2000). Attentional capture and inattentional blindness. *Trends in Cognitive Sciences*, **4(4)**, 147-155.

Frischer, G., Zeilon, R., Mattsson, L., & Parkbring, S. (2011). Selective attention test. (video available at http://www.youtube.com/ watch?v= dbjPnXaacAU)

Simons, D.J., & Chabris, C.F. (1999). Selective attention test. (video available at http://www.youtube.com/watch?v=vJG698U2Mvo)

Syntonic and eye accommodation changes

Evita Serpa[1]*, Ruggero Consonni[2], Gunta Krumina[1]

[1] *University of Latvia, Faculty of Physics and Mathematics, Department of Optometry and Vision Science, Riga, Latvia*; [2] *OptiVist, Casteggio (PV), Italy*

E-mail: evita.serpa@gmail.com

Introduction

Light as a therapeutic agent has been used for a very long time. Clinical research in the last decades showing the impact of light on cells, blood, circadian rhythms, and mood disorders has increased the acceptance of light as a therapeutic agent (*Gottlieb & Wallace*, 2010). Syntonic is the method of vision therapy in which treatment is performed using specific light frequencies entering the eye. It is believed that chronic systemic, mental/emotional, and visual ailments are caused by the imbalance of autonomic nervous and endocrine system and specific lights frequencies entering the eye are making balance in mentioned systems (*Spitler*, 1941). Eye accommodation is directly related to the autonomic nervous system. The aim of our study is to get a better understanding of the syntonic effect on eye accommodation functions observing treatment results of subjects with different disorders who receive syntonic treatment. So far there are not many studies in this field. One of the studies shows accommodative ranges improvement after treatment with light therapy (*Anikina et al.*, 1995).

Method

The research included 20 presbyopic subjects of age between 40-50. Selected subjects were divided into two subgroups: the control group (10 subjects) that didnt perform the syntonic exercises, and the syntonic group (10 subjects) that performed the syntonic exercises. The syntonic group received the 20 days treatment. To investigate the possible effect of syntonic treatment on presbyopic subjects, the attention was focused on the analysis of the near additive, accommodative amplitude, near visual acuity, and visual functional field to investigate any changes on these aspects before and after the exercises.

Results

Syntonic group demonstrated statistically significant improvement (p=0.002) in visual acuity and statistically significant improvement (p<0.05) in individual visual functional field analysing form, green and blue functional field. Analysing accommodation function, reduction in addition power has been observed of 40% of the syntonic group participants and 30% participants have increased their accommodation amplitude after syntonic exercise performing.

Conclusion

These results indicate that syntonic is a powerful instrument to act in the young subjects with presbyopia. Moreover, the study of visual functional field is the most sensitive and accurate way to evaluate progresses in visual training and all these aspects are important for the balance system.

References

Gottlieb, R.L., & Wallace, L.B. (2010). Syntonic phototherapy. *Photomedicine and Laser Surgery*, 28(4), 449-452.

Anikina, E.B., Avetisov, E.S., Gubkina, G.L., Khoroshilova-Maslova, I.P., & Shapiro, E.I. (1995). Applying lasers to accommodation disorders. *Laser Physics*, 5, 917-921.

Spitler, H.R. (1941). *The syntonic principle*. College of Syntonic Optometry, Eaton.

Optical materials and phenomena: talks

All-organic optical waveguide devices for communication and sensing applications

Edgars Nitiss, Andrejs Tokmakovs, Janis Alnis, Janis Busenbergs, Martins Rutkis

Institute of Solid State Physics, Laboratory of Organic Materials

E-mail: edgars.nitiss@cfi.lu.lv

In the last couple of decades a tremendous growth in the use and development of waveguide photonics in the measurement technology and informatics can be noticed. This has been motivated mainly by the requirements in miniaturization of devices as well as in reduction of their costs and energy consumption. In this presentation we demonstrate our achievements in creation and characterization of all-organic waveguide devices made using direct-write optical lithography. We have used both positive and negative resists for the creation of passive elements, such as bends and resonators, and active devices such as electro-optic modulators. We will discuss the principles of the development of previously mentioned elements as well as strategies for device testing.

Structural investigations of thermochromic phase transition in copper molybdate

Inga Jonane[1,*], Arturs Cintins[1], Aleksandr Kalinko[2], Roman Chernikov[3], Alexei Kuzmin[1]

[1] *Institute of Solid State Physics, Kengaraga 8, Riga, Latvia, LV-1063*

[2] *Universität Paderborn, Naturwissenschaftliche Fakultät, Department Chemie, Warburger Strasse 100, 33098 Paderborn, Germany*

[3] *DESY Photon Science, Notkestraße 85, D-22607 Hamburg, Germany*

[*]*E-mail:* inga.jonane@cfi.lu.lv

Copper molybdate ($CuMoO_4$) is an interesting functional material exhibiting thermochromic and piezochromic properties [1]. Significant changes in molybdate structure and optical properties due to the temperature and/or pressure treatment make it a perspective material for a wide range of chromic-related applications, starting from the user-friendly temperature and pressure indicators to "smart" inorganic pigments.

At ambient pressure and below room temperature, $CuMoO_4$ exists in two phases: brownish-red γ-$CuMoO_4$ and green α-$CuMoO_4$ [1]. First order phase transition from γ-to-α-phase occurs in the temperature range between 175 K and 260 K [2]. In both phases $CuMoO_4$ remains in triclinic $P\bar{1}$ symmetry [1], but the local environment differs significantly. γ-$CuMoO_4$ is built up of distorted CuO_6 and MoO_6 octahedra. α-$CuMoO_4$ is composed of distorted CuO_6 octahedra, CuO_5 square-pyramids and distorted MoO_4 tetrahedra (Figure 1).

To follow the evolution of the local structure in $CuMoO_4$ during the phase transition, we performed low temperature (10-300 K) X-ray absorption spectroscopy study at the Cu and Mo K-edges. The analysis of the Mo K-edge X-ray absorption near edge structure (XANES) allowed us to follow the phase transition, tracing a variation of the pre-edge shoulder [3]. At the same time, the extended X-ray absorption fine structure (EXAFS) analysis allowed us to reconstruct the radial distribution functions and to characterize structural changes around Mo and Cu atoms.
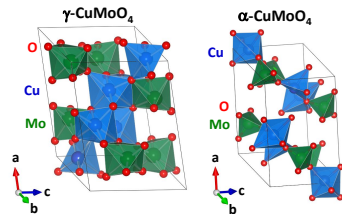

Figure 1: Crystallographic unit cells of low-temperature γ-$CuMoO_4$ and high-temperature α-$CuMoO_4$ phases.

References

[1] M. Wiesmann, H. Ehrenberg, G. Miehe, et al., J. Solid State Chem. 132, 88 (1997)

[2] M. Gaudon, C. Carbonera, A. E. Thiry, et al., Inorg. Chem. 46, 24 (2007)

[3] I. Jonane, A. Cintins, A. Kalinko, et al., Low Temp. Phys. 44 (2018)

Energy transfer in Dy^{3+}/Eu^{3+} co-doped glasses and glass-ceramics containing fluoride nanocrystallites

Meldra Kemere[*], Uldis Rogulis

Institute of Solid State Physics, Kengaraga 8, Riga, Latvia, LV-1063
[*]*E-mail:* meldra.kemere@gmail.com

Rare earth (RE) ions doped oxyfluoride glass-ceramics have been widely investigated in the last decades due to their potential applications in sensors, scintillators, infrared detectors and lighting sources. The advantage of oxyfluoride glass ceramics lies in the ability to alter and increase the luminescence intensity of dopant ions if they substitute cations in the fluoride nanocrystals.[1] However, optical properties depend strongly on the local structure around RE ions.

Dy^{3+} doped materials are widely used in optical devices, including white light phosphors. Adding of Eu^{3+} ions can improve the colour properties of the emitted light.[2] In the present study, luminescence of europium and dysprosium co-doped glass-ceramics containing SrF_2 nanocrystallites has been investigated and analysed in comparison to the previously obtained results.

In the present study, oxyfluoride glasses with the composition SiO_2-Al_2O_3-Na_2O-SrF_2, activated with Dy^{3+} and Eu^{3+} ions (0-2 mol%) have been synthesized. The obtained glasses were annealed at 650, 700 and 750 °C temperature (1 to 4 hours) to obtain glass-ceramics containing SrF_2 nanocrystallites. Luminescence emission, excitation and decay measurements have been made. The obtained results were compared with the previous series of composition SiO_2-Al_2O_3-CaO-CaF_2.

In the glass-ceramics, luminescence lifetimes of Dy^{3+} ions have increased compared to the precursor glasses. This result indicates that a part of rare earth ions have been incorporated in SrF_2 nanocystallites. In comparison with the CaF_2 containing samples, the samples with SrF_2 nanocrystallites show longer luminescence lifetimes, but the energy transfer efficiency is lower. The energy transfer efficiency and its impact factors in both series were analysed. The colour properties of the emitted light and their validity for white light sources were analysed.

References

[1] P.P. Fedorov, A. A. Luginina, A. I. Popov, Transparent oxyfluoride glass ceramics, J.Fluorine Chem. **172**, 22-50 (2015)

[2] Rajesh, D., Brahmachary, K., Ratnakaram, Y. C., Kiran, N., Baker, A. P., Wang, G. G.,Energy transfer based emission analysis of Dy^{3+}/Eu^{3+} co-doped ZANP glasses for white LED applications, Journal of Alloys and Compounds, **646**, 1096-1103 (2015)

Multisite formation in Gd^{3+} and Eu^{3+} doped SrF_2 nanoparticles

Andris Antuzevics, Meldra Kemere, Guna Krieke

Institute of Solid State Physics, Kengaraga 8, Riga, Latvia, LV-1063

*E-mail: andris.antuzevics@gmail.com,

Fluoride materials can act as ideal rare earth (RE) hosts due to the low phonon frequencies that are crucial for efficient luminescent performance. Due to a growing interest in nanostructured materials, characterization of nano-sized fluorides is of great fundamental and practical importance.

The relatively simple cubic fluorite structure of SrF_2 provides a great diversity of sites for trivalent impurities. There are multiple ways to ensure charge neutrality when a RE^{3+} ion substitutes the Sr^{2+} ion and each position leads to different optical properties. In this work we use Gd^{3+} and Eu^{3+} ions as spectroscopic probes to analyse the formation of different centres in SrF_2 nanoparticles.

SrF_2 nanoparticles doped with gadolinium and europium ions were synthesized using the precipitation method. Afterwards the samples were annealed at different temperatures in either air or argon atmosphere. X-ray diffraction, scanning electron microscopy and transmission electron microscopy measurements were made to verify the nanocrystallinity of the studied samples.

Analysis with magnetic resonance and optical spectroscopy techniques revealed that the local structure around the probe in highly dependent on the heat treatment procedure. Based on electron paramagnetic resonance and optical spectra the different site symmetries have been identified.

PHOTOLUMINISCENCE AND AMPLIFIED SPONTANEOUSE EMISSION OF NEAT 4H-PYRAN DERIVATIVE CONTAINING THIN FILMS

Julija Pervenecka[1]*, Aivars Vembris[1], Elmars Zarins[2], Valdis Kokars[2]

[1]*Institute of Solid State Physics, Kengaraga 8, Riga, Latvia, LV-1063*
[2]*Institute of Applied Chemistry, Riga Technical University*
E-mail: julija.pervenecka@inbox.lv,

Organic solid-state lasers are one of in nowadays perspective and intensively developing technology in which as laser dyes are widely used different non crystalline structure films forming organic molecules. As all lasers organic solid-state laser should also consists from two main elements: an active medium and resonator. In comparison with traditional inorganic lasers, they would be much cheaper and more easily integrated into photonic devices [1].

However, not all organic compounds could be used for laser active medium preparation. The main requirement for the compound is possibility to excite amplified spontaneous emission (ASE) in their thin films. Only materials, which appropriate to this requirement can be used for preparation of a laser active medium.

In this work were investigated photoluminescence and amplified spontaneous emission properties of one original 4H-pyran derivative(E)-5-(2-(4-(bis(2-(trityloxy)ethyl)amino) styryl)-6-methyl-4H-pyran-4-ylidene)-1,3-dimethylpyrimidine-2,4,6(1H,3H,5H)-trione (MWK-1) that form amorphous thin films from solution. MWK-1 is newly synthesised original non-symmetric chromophore molecule that absorbs light in beginning till middle of visible spectral range (375 nm-575 nm) with maximum at 491 nm and emits it within red spectral region.

Thin films of investigated compounds on glass substrate were made from chloroform solution by the spin- coating method.

Photoluminescence was excited at MWK-1 absorption maximum wavelength: 491 nm. Emitted spectrum was Stokes shifted by   203 nm, full width at half maximum of the photoluminescence was   145 nm, maximum at 694 nm. Amplified spontaneous emission was excited by Ekspla 310 series pulse laser at 491 nm wavelength. The irradiation area on the surface of the sample was stripe form with dimension 3×0.4 mm^2. Light emission was collected at the edge of the sample and measured by spectrometer OceanOptics HR4000. As havent been expected, ASE peak was blue-shifted from PL maximum (approximately by 21 nm). Full width at half maximum of the ASE was   10 nm with maximum position at 673 nm. Amplified spontaneous emission threshold energy was 65,22 μJ/cm^2.

In my presentation I will discussed about photoluminescence and ASE properties of MWK-1 pure thin films and its perspectives for future use as laser dye in red lasers.

References:
[1] Sebastien Forget, Sebastien Chenais, *"Organic Solid-State Lasers"*, Springer-Verlag Berlin Heidelberg 2013, Volume 175, p. 179

Optical materials and phenomena: posters

Dark Field Optical Spectroscopy of Deposited Ag Nanocube Arrays and their Raman Enhancement

Mindaugas Juodenas[1,*], Tomas Tamulevicius[1,2], Juris Prikulis[3], Donats Erts[3], Adrien Chauvin[4], Abdel-Aziz El Mel[4], Sigitas Tamulevicius[1,2]

[1] *Institute of Materials Science, Kaunas University of Technology, K. Barsausko St. 59, Kaunas, Lithuania, LT-51423*
[2] *Department of Physics, Kaunas University of Technology, Studentu St. 59, Kaunas, Lithuania, LT-51368*
[3] *Institute of Chemical Physics, University of Latvia, Jelgavas St. 1, Riga, Latvia, LV-1004*
[4] *Jean Rouxel Institute of Materials, University of Nantes, 2 Chemin de la Houssinire, Nantes, France, 44300*
E-mail: mindaugas.juodenas@ktu.lt

Nanoparticles of noble metals have been receiving a lot of attention lately. That is mainly because of a joint effect of the nanotechnology enabled by the small size and unique shape of these tiny objects [1] and the interesting and useful optics due to the nature of such metals [2]. Often new effects can be demonstrated when nanoparticles are deposited into well-defined regular arrays [3].

In this work we have used capillary force assisted nanoparticle assembly technique [4] to deposit Ag nanocubes into regular arrays. This technique allows for precise control of the deposition yield through the parameters of the process, i.e. temperature, velocity, etc. Briefly, a miniscule amount of colloid nanoparticle solution is constrained between a glass slide and a corrugated surface, which is translated at a velocity and held at a constant temperature. The balance between evaporation and laminar flow based fluxes within the droplet cause a well-controlled and high-yield deposition of nanoparticles.

We have investigated such arrays using dark field microscopy and optical spectroscopy and found interesting effects of scattered light depending on the geometry of nanoparticle assemblies. Additionally, we performed finite element simulation analysis which explained the scattering properties of the particle assemblies pretty well. Furthermore, Raman scattering enhancement of model organic molecule on such noble metal nanoparticle arrays was demonstrated. These results are expected to be used for extra-high sensitivity bio-sensors.

References
[1] Flauraud V. et al, Nature Nanotechnology **12**, 73-80 (2017)
[2] Peckus D. et al., The Journal of Physical Chemistry C **121**, 24159-24167 (2017)
[3] Henzie J. et al., Nature Materials **11**, 131-137 (2012)
[4] Virganavicius D. et al., Applied Surface Science **406**, 136-143 (2017)

Metal oxide – Silicon 1D Nanocomposites as effective platform for optical applications

M. Pavlenko[1], R. Viter[2], S. Jurga1[1], I. Iatsunskyi[1*]

[1] *NanoBioMedical Centre, Adam Mickiewicz University, 85 Umultowska Str., 61-614, Poznan, Poland*
[2] *Institute of Chemical Physics, and Institute of Atomic Physics and Spectroscopy, University of Latvia, 19 Raina Boulevard, LV 1586 Riga, Latvia*
E-mail: yatsunskiy@gmail.com,

In recent years, one-dimensional nanostructures such as nanofibers, nanowires and nanopillars attract much attention as prominent material for optical applications. Due to high surface area and eligibility to control optical and electronic properties, 1D nanostructures are widely used in energy-harvesting materials such as photoelectrodes, solar cells, photocatalysts, etc [1]. Silicon as a cheap and abundant material, which suitable for simple chemical processing and wide range of doping represents an obvious choice for application in photovoltaics and photonics. Well-developed method of metal-assisted chemical etching (MACE) allows fabrication of wire/pillar arrays with different structural and morphological properties. Combination of such arrays with additional layers of metal oxides (e.g. TiO2, ZnO) leads to effective tuning of optical properties (e.g. enable to enhance the absorbance in wide range of wavelength including the visible range). Due to effective light absorbance and, therefore, low reflectance metal oxide (MOx) – Si 1D nanostructures represent a good base for building the efficient solar cell [2]. On the other hand, MOx-Si 1D nanostructures allow one to tune photoluminescence properties what is extremely important for development of novel composites for optical (bio)sensor applications. In present study, our group used the previously developed technique conceived of MACE in combination with atomic layer deposition (ALD) for deposition of different metal oxides (TiO2 and ZnO). The influence of ZnO and TiO2 phase and morphology on the optical properties of fabricated 1D nanocomposites were investigated by means of Raman spectroscopy, UV-VIS, reflectance and photoluminescence measurements. In conclusion, studying and analysis of obtained data revealed strong dependence of optical properties on the composition and structure of core-shell silicon-MOx 1D nanostructures. We have also shown that these nanocomposites can be used as effective platform for optical biosensors and photoanodes for solar water splitting processes.

Acknowledgements

References

[1] Mykola Pavlenko, Katarzyna Siuzdak, Emerson Coy, Igor Iatsunskyi, et al., International Journal of Hydrogen Energy **Volume 42(51)**, 30076-30085 (2017)
[2] Dae-Yeong Lee1, Hyunjin Kim, Hua-Min Li, et al., Nanotechnology **Volume 24(17)**, 2013

Super-light metainterfaced plasmon-polaritons

Yaraslau Zubrytski[1,*]

[1]*Physical Department, Division of Physical Optics,
Belarusian State University, Minsk, Belarus (student)*
[*]*E-mail:* yauz_lv@inbox.lv

The recent experiments showed that both phase and group velocities of the wave that passes through the metamaterial can posses both negative and positive sign [1]. Besides, the interface excitations can exhibit superluminal behaviour. Such features are of fresh practical interest for the design of electromagnetic transformation devices, e. g., antennas.

The present work brings a simple design of and revealing the superluminal properties of plasmon-polaritons at the interface of hyperbolic metamaterial and external dielectric medium. For the system envisaged the effective medium theory results in the next dielectric function tensor component of the PPs propagating along the x-axis:

$$\epsilon_x = \epsilon_{out}\epsilon_{zz}(\epsilon_{out} - \epsilon_{xx})/(\epsilon_{out}^2 - \epsilon_{xx}\epsilon_{zz}), \tag{1}$$

where ϵ_{out} is the dielectric permittivity of the external medium, e. g. SiO_2, ϵ_{xx}, ϵ_{zz} are the transverse and longitudinal tenzor components. Refractive index of an external medium, volume fraction δ of the guest medium within the MM serviced as variables.

From Fig. 1 one can see that superluminal feature imaginate in wide tuned spectral range. An absolute value of the phase velocity can exceed light velocity up to 4 times. Its scaling can spread one order of magnitude. Superluminal feature coexist with extra subluminal one that looks like trapping and suggests memory design. In the validity point of view one can write relationship between the phase and group velocities as:

$$1/\Re(v_g) + 1/\Re(v_{ph}) = \zeta\Re(n)/c, \tag{2}$$

where ζ takes value of 2 while the dispersion laws for the dielectric and magnetic functions are similar. One sees, the binding protects velocity overflow in both the value and sign, and the negative value (not backwarded) can correspond to the pulse reshaping.
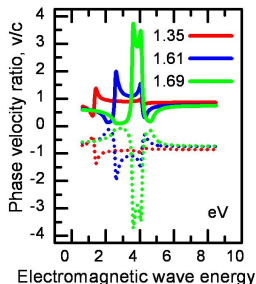

Figure 1: TiO$_2$/Ag's v_{ph} spectral dynamics.

References

[1] G. Dolling, C. Enkrich, M. Wegener, C. M. Soukoulis, S. Linden, Science, **312**, 892 (2006)

Biophotonics: talks

Application of optical tweezers for examination of mutual interaction of red blood cells with nano-materials

Igor Meglinski

University of Oulu, Biophotonics group, Opto-Electronics and Measurement Techniques Laboratory

E-mail: igor.meglinski@oulu.fi,

The application of red blood cells (RBC) as natural transport agents for systemic drug delivery either encapsulated in the cell's inner volume, or coupled to the surface of RBC is considered as a new paradigm in modern medicine that possesses a great potential. To reveal possible undesirable effects in routine delivery of synthetic nano-materials by RBC in day-to-day clinical practice an ultimate understanding of their mutual interaction is required. Mutual interactions of RBC incubated with various nano-materials were assessed by using optical tweezers (OT) and validated by scanning electron microscopy (SEM). The experiments are performed in a platelet-free blood plasma mimicking natural conditions. The results demonstrate that OT provides high precision measurements of RBC interaction at a pico-newton (pN) scale, whereas SEM imaging shows localization of nano-materials on the RBC membranes.

Non-invasive optical skin evaluation device for cancer screening

Marta Lange[1], Dmitrijs Bliznuks[2], Alexey Lihachev[1,*], Emilija Vija Plorina[1,*], Ilze Lihacova[1,*], Janis Spigulis[1,*]

[1] *Biophotonics Lab, Institute of Atomic Physics and Spectroscopy, University of Latvia, Skunu Street 4, Riga, Latvia*
[2] *Riga Technical University, Kalku Street 1, Riga, Latvia*
* E-mail: marta.lange.rtu@gmail.com,

Skin cancer is an increasing problem worldwide. A diagnostic tool is essential for dermatologists and primary-care doctors for skin screening. For this reason, an optical, non-invasive, inexpensive diagnostic device has been created. The setup consists of camera, LEDs arranged in a ring around the camera sensor and a computer for data processing. Light sources include three narrow bandwidth LEDs: 525nm, 660nm and 940nm for diffuse reflectance, as well as 405nm LED for to induce skin autofluorescence (AF).[1][2] After the acquisition of clinical images, the device is capturing a set of images and transfers them to cloud based diagnostic service (scalable Matlab computing nodes). That allows virtually unlimited processing power for diagnosis calculations and the ability to access diagnosis through the internet by using any personal computer or smartphone. With the proposed system [3] it is possible to distinguish different skin malformations, for instance, regular nevi, seborrheic keratosis, melanoma and to evaluate the post-operative scars for possible tumor recurrence. The analysis is based on AF and p criterion – characterization of the proportion of hemoglobin and melanin in the skin sensitive for melanoma recognition from other pigmented skin formations.[4] This optical and non-invasive device has been successfully tested on a clinical setting; the algorithm is still being improved for more types of dermatological diseases to be distinguished for diagnostic screening purposes.

References

[1]Diebele, I., Kuzmina, I., Lihachev, A., Kapostinsh, J., Derjabo, A., Valeine, L., Sigulis, J., "Clinical evaluation of melanomas and common nevi by spectral imaging", Biomedical Optics Express 3(3), 67-472 (2012)

[2]Lihachev, A., Derjabo A., Ferulova, I, Lange, M., Lihacova I., Spigulis, J., "Autofluorescence imaging of basal cell carcinoma by smartphone RGB camera", J. of Biomedical Optics, 20(12), 120502 (2015)

[3]Bliznuks D., Jakovels D., Saknite I., Spigulis J. Mobile platform for online processing of multimodal skin optical images // International Conference on BioPhotonics, 2015, pp. 1-4, DOI: 10.1109/BioPhotonics.2015.7304024

[4]Lihacova, I. "Evaluation of skin oncologic pathologies by multispectral imaging methods", Summary of Doctoral Thesis, University of Latvia, 2015. ISBN nr: 978-9984-45-997-4.page 30.

Method for skin disease classification using skin autofluorescence imaging

Emilija Vija Plorina[1,*], Ilze Oshina[1], Marta Lange[1], Ilze Lihacova[1], Alexander Derjabo[1], Alexey Lihachev[1]

[1]*Institute of Atomic Physics and Spectroscopy, University of Latvia, Riga, Latvia*
*E-mail: evplorina@gmail.com,

Over the last decades the incidence of malignant skin diseases such as basal cell carcinoma (BCC), squamous cell carcinoma (SCC) and malignant melanoma (MM) have been increasing in incidence in light-skinned populations [1]. Even less dangerous types of skin cancer have a large negative impact on the quality of life of the patients [2]. Since the number of state funded specialists is limited, it is crucial that diagnostic devices for primary care physicians are developed. In this study we used autofluorescence imaging for the classification of benign and malignant skin diseases. Excitation of the skin tissue was achieved using narrow band 405 nm LED illumination using a non-invasive imaging device which has been tested to be effective for skin disease imaging in previous studies [3]. A RGB camera inside the device sends the captured images to a computer which then can be subsequently processed. The green channel of the image is used as the excitation wavelength causes skin tissue autofluorescence that is most pronounced in this RGB channel. The most important classification aims were to differentiate melanoma from other pigmented skin lesions, namely nevi and pigmented basal cell carcinomas, as well as to differentiate basal cell carcinoma from similar looking benign skin diseases such as keratoses, psoriasis, dermatofibroma etc. Moreover, the autofluorescence intensity of skin diseases compared to healthy skin of the subject is used as a potential assessment parameter. The sensitivity and specificity for the differentiation will be analysed. The potential diagnostic accuracy of the approach will be evaluated and presented.

References

[1] Apalla, Z., Nashan, D., Weller, R.B., and Castellsagu, X., Skin Cancer: Epidemiology, Disease Burden, Pathophysiology, Diagnosis, and Therapeutic Approaches, Dermatology and Therapy, 7(Suppl 1):5-19 (2017).

[2] BurdonJones, D., Thomas, P. and Baker, R., Quality of life issues in nonmetastatic skin cancer, British Journal of Dermatology, 162: 147-151 (2009).

[3] Lihachev, A., Derjabo, A., Ferulova, I., Lange, M., Lihacova, I., Spigulis, J., Autofluorescence imaging of Basal Cell Carcinoma by smartphone RGB camera, J. Biomed. Opt. 20(12): 120502.

Biophotonics: posters

Double snapshot mapping of skin chromophores at triple and double wavelength illumination.

Raimonds Ciems[1,*], Ilze Osina[2], Janis Spigulis[2]

[1]*Biophotonics Laboratory, Institute of Atomic Physics and Spectroscopy, University of Latvia, 19 Rainis Blvd., Latvia, Riga, LV-1586*

[*]*E-mail:* raimonds.ciems@gmail.com,

Development of non-invasive medical devices opens doors for a quicker and more efficient disease detection and diagnostics.

The aim of this work is to develop a program which could process images taken by illuminating skin pathology with five different wavelength lasers. And further, to calculate chromophore maps from processed pictures.

Skin pathology is photographed with the device, which takes two pictures in short amount of time. The first image is obtained by illuminating skin with three different lasers with wavelengths 450 nm, 526 nm and 850 nm. Lasers used for the second image are with wavelengths 406 nm and 656 nm. Then images are sorted in R, G and B output values. Two more images, obtained by illuminating white sheet with corresponding wavelengths, are sorted in output values. Thus, there are 21 images and from their matrix value attenuation coefficients can be calculated. When combining attenuation and chromophore extinction coefficients, as well as wavelengths and chromophore concentrations, chromophore maps can be obtained using Beer-Lambert law [1]:

$$
\begin{cases}
c_a \cdot \varepsilon_a(\lambda_1) + c_b \cdot \varepsilon_b(\lambda_1) + c_c \cdot \varepsilon_c(\lambda_1) + c_d \cdot \varepsilon_d(\lambda_1) + c_e \cdot \varepsilon_e(\lambda_1) = -\frac{lnk_1}{l_1} \\
c_a \cdot \varepsilon_a(\lambda_2) + c_b \cdot \varepsilon_b(\lambda_2) + c_c \cdot \varepsilon_c(\lambda_2) + c_d \cdot \varepsilon_d(\lambda_2) + c_e \cdot \varepsilon_e(\lambda_2) = -\frac{lnk_2}{l_2} \\
c_a \cdot \varepsilon_a(\lambda_3) + c_b \cdot \varepsilon_b(\lambda_3) + c_c \cdot \varepsilon_c(\lambda_3) + c_d \cdot \varepsilon_d(\lambda_3) + c_e \cdot \varepsilon_e(\lambda_3) = -\frac{lnk_3}{l_3} \\
c_a \cdot \varepsilon_a(\lambda_4) + c_b \cdot \varepsilon_b(\lambda_4) + c_c \cdot \varepsilon_c(\lambda_4) + c_d \cdot \varepsilon_d(\lambda_4) + c_e \cdot \varepsilon_e(\lambda_4) = -\frac{lnk_4}{l_4} \\
c_a \cdot \varepsilon_a(\lambda_5) + c_b \cdot \varepsilon_b(\lambda_5) + c_c \cdot \varepsilon_c(\lambda_5) + c_d \cdot \varepsilon_d(\lambda_5) + c_e \cdot \varepsilon_e(\lambda_5) = -\frac{lnk_5}{l_5}
\end{cases}
\tag{1}
$$

As a result, in short amount of time five chromophore maps are obtained – oxyhemoglobin, deoxyhemoglobin, melanin, bilirubin and lipids. These maps provide relative information about hemoglobin content in blood, relative amount of melanin and relative concentration of bilirubin. In case of melanin, it allows to establish cancerous lesions on the skin, while bilirubin concentrations allow to follow up healing dynamics of a bruise.

Motion artifacts and different thickness of human skin throughout the body affects reliable results. Therefore, stabilization algorithm and different mean photon path length in skin is used when chromophore maps are calculated.

References
[1]Express RGB mapping of three to five skin chromophores / Ilze Oshina, et. al., Optics InfoBase Conference Papers Munich, 2017 Vol. Part F61-ECBO 2017 (2017), 1-5 p.

Remote photoplethysmography method for skin monitoring on layers of different depths.

Roberts Kaķis[1,*], Uldis Rubīns[1]

[1]*Biophotonics Laboratory, Institute of Atomic Physics and Spectroscopy, University of Latvia, Raina blvd 19, Riga, LV-1586, Latvia*
E-mail: robertskakis@gmail.com,

Remote photoplethysmography is contactless subtype of photoplethysmography. This method is used to reflect palmar microcirculation changes during various external provacations such as heating liniment application, blood pressure cuff using, cold-heat test realization. The experimental device consists of two LED illuminators of different wavelengths: infrared (810nm) and green (530nm); a CMOS sensor that detects reflected light and a computer with MATLAB software that analyses and displays changes of microcirculation amplitude in skin regions. This system observes changes during the above-mentioned tests. From the obtained data, it is possible to calculate the perfusion index in various parts of skin. By evaluating perfusion index it is possible to determine whether a person has a tissue bleeding disorder. The purpose of the study is to verify in practice whether the results are consistent with theoretical assumptions.

ESTIMATION OF POTENTIAL SUSTAINABILITY OF WOODY PLANT SPECIES TO STRESSFUL ENVIRONMENTAL FACTORS BY INDUCTION CHLOROPHYLL FLUORESCENCE

Nesterova N.[1,*], Sychuk A.[2], Illienko V.[1], Ruban Yu.[1], Shpyrka N.[1], Pareniuk O.[1], Shavanova K.[1]

[1] *National University of Life and Environmental Sciences of Ukraine Heroyiv Oborony st., 15, Kyiv-03041, Ukraine*
[2] *Institute of Plant Physiology and Genetics of NAS of Ukraine Vasylkivska st., 15/31, Kyiv-03042, Ukraine*
[*] *E-mail:* koriza@ukr.net,

This paper deals with the results of the photosynthetic apparatus tests of 11 woody plant species that grow in different ecological conditions of the city Kyiv using the portable device "Floratest". This method gives an opportunity to evaluate the range of effective functioning of photosystem 1 and 2 under stressful environmental factors, and damage and subsequent restoration of the photosynthetic apparatus itself.

We aimed to investigate the functioning of the photosynthetic apparatus of woody plants in the urbanized environment. Conventionally clean zone, the National Botanical Garden of M.M. Grishko, was used as a control. As zone 2 we used parklands with minimized stress, zone 3 - plantations along highways with intensive traffic. We used leaves of 20-30-year-old trees, 10 pieces in each repetition.

As a result, we showed that the highest potential resistance to stress factors within zone 3 had *Aesculus carnea, Populus nigra* L. and *Robinia pseudoacacia* L. plants. While, for parklands, while using relevant agro-technology, it is advisable to use *Quercus robur* L., *Acer saccharum* Marsh and *Tilia cordata* Mill plants. Other species, in particular, *Aesculus hippocastanum* L., *Acer platanoides* L. and *Betula pendula* Roth showed low resistance to stress factors in all studied areas.

An algorithm for speckle effect minimization in endoscopic optical coherence tomography

Anton Potlov*, Sergey Frolov, Sergey Sindeev, Sergey Proskurin

Biomedical Engineering, Tambov State Technical University, Sovetskaya 106, Tambov, Russia, 392000

*E-mail: zerner@yandex.ru

High-quality optical coherence tomography (OCT) structural images reconstruction algorithm for endoscopic OCT of soft biological tissue is described [1, 2]. The key feature of the algorithm is combination of multilevel filtering and raster scanning in sample arm with consecutive averaging.

Multilevel filtering of experimental OCT raw data includes:

1) thresholding with a predetermined threshold limit value for the intensity of the interference signal and band-pass filtering with a predetermined upper and lower cut-off frequency. These operations, preliminary, allow reducing the noise for a number of adjacent A-scans;

2) morphological image processing for B-scans (structural OCT images) for reducing speckle noise level;

3) median filtering with a given left and right rank for smoothing the resulting image.

The speckles geometry (the result of mutual interference of waves reflected back from the structures of an investigated biomedical object) of a structural OCT image [3] is different from the one appeared using standard scanning. Each time speckles are formed perpendicular to the radiation beam, which probes an investigated biological tissue at different angles. Such speckle geometry makes raster averaging especially effective. The structural OCT image split into non-overlapping spatial column blocks. Adjacent column blocks are averaged pixel-by-pixel forming a new structural image. This image is splitted into non-overlapping spatial row blocks. Adjacent row blocks are averaged pixel-by-pixel forming a completely averaged structural image. The process of raster averaging of structural image is controlled by the analytically established exponential mathematical relationship of the size (in bytes) of a file of the averaged structural image on the number of raster averaging. This approach allows reducing speckle noise, improve S/N ratio and, at the same time, minimize size of the file of the structural image itself [2].

The proposed algorithm is characterized by high speed of raw data processing and optimal size of the files of resultant structural images. The described algorithm allows for obtaining high-quality structural images of an investigated soft biological tissue in the otorhinolaryngology, gastroenterology, urology, gynecology in vivo using endoscopic OCT.

Acknowledgements

References

[1] Frolov, S.V. et.al. Quantum Electronics. **47(4)**, 347354 (2017).
[2] Frolov, S.V. et.al. Proceedings of SPIE. **10336**, 103360Z (2017).
[3] Gora, M.J. et.al. Biomedical Optics Express. **8(5)**, 24052444 (2017).

Laser physics and spectroscopy: talks

Spin Detection using Nitrogen-Vacancy Centres in Diamond

Florian Helmuth Gahbauer

University of Latvia, Department of Physics, Laser Centre
E-mail: florian.gahbauer@lu.lv,

Nitrogen-vacancy (NV) centres in diamond have been used to detect spins on the surface of a diamond and even to perform nuclear magnetic resonance experiments on nanoscale samples. We will describe the technique and recent work and discuss ongoing research into possible applications.

Third-order nonlinear optical properties of thin organic films and solutions

Arturs Bundulis*, Edgars Nitiss, Martins Rutkis

Institute of Solid State Physics, Kengaraga 8, Riga, Latvia, LV-1063

* E-mail: bundulis.arturs@gmail.com,

Due to the fast development of telecommunication industry, all-optical data processing, transmission and storage devices has attracted a great interest. Although concepts for such devices already exist, their implementation is delayed due to difficulties of finding materials with necessary third-order non-linear optical (3oNLO) properties. Nowadays scientist mainly focuses on organic molecules due to their high potential for NLO applications. Main advantage of organic materials is the possibility to easily modify their molecular structure to acquire desired optical properties. In this work we studied 3oNLO parameters Kerr effect and two-photon absorption - of several aminobenziliden-1,3-indandione.

To evaluate 3oNLO properties of our molecules we implemented Z-scan method using picosecound (ps) and nanosecound (ns) Nd:YAG 1064 nm lasers. Measurements were carried out for solutions with organic compounds dissolved in chloroform and thin films with host-guest system with PMMA as host. While measuring nonlinear refractive index of our materials with ns laser we concluded that thermal effects induced in chloroform can lead to overestimation of Kerr effect magnitude while studying our samples in a form of solution. To evade such error, it is important to choose correct experimental parameters laser pulse length and frequency. Using ps laser we analyzed Kerr and two-photon absorption effects.

Theoretical insights into the electronic structure and low-lying states of the uranium nitride molecule

Darya Meniailava[*], Maksim Shundalau

Physiscs Faculty, Belarusian State University, Nezavisimosti Ave. 4, Minsk, Belarus, 220030

[*]*E-mail:* meniailava@bsu.by,

Disadvantages of nuclear oxide fuel stimulate interest in the development and study of new alternative fuels. Promising and potentially important analogues are carbide and nitride uranium fuels, which are used for fast reactors and have a number of advantages (higher thermal conductivity, higher density of metal atoms, less radiotoxicity versus oxides, etc.). For the safe use of such fuel, it is necessary to know its thermodynamic characteristics, which are uniquely related to molecular parameters. Uranium mononitride is less studied experimentally and theoretically. Within the theoretical approach electronic states of the UN molecule were studied at DFT [1-2] and some molecular spectroscopic constants were obtained.

In this study, the calculation of the complete potential energy (PECs) curves of the low-lying electronic states of the UN molecule was carried out for the first time and the spectral, energy, dynamic and other characteristics of their vibronic states were determined. The calculations were performed within multi-reference perturbation theory approximation CASSCF/XMCQDPT2 [3], taking into account spin-orbit coupling (SOC). To describe the uranium atom, relativistic Stuttgart ECP80 pseudopotential (internal electrons) and TZ-basis (external electrons) were used, the nitrogen atom - full-electron TZ-basis set. The active space for CASSCF calculations consisted of 7 electrons in 9 orbitals. The state-averaged procedure was carried out for 10 low-lying doublet ($S = 1/2$) and 10 quartet ($S = 3/2$) states for UN. The calculations were performed pointwisely in the internuclear distances range of 1.5-8.0 Å. Further, in order to correct the PECs, we performed calculations in the multi-reference perturbation theory approximation XMC-QDPT2. The SOC was also carried out by perturbation theory using the Pauli-Breit operator. To determine the accuracy of the calculations we compared the calculated energies of molecular states at the dissociation limits (at the internuclear distance of 8.0 Å) with the sum of the experimental energies [4] of separated uranium and nitrogen atoms.

References

[1] D. W. Greenand, G. T. Reedy, J. Chem. Phys. **65**, 2921-2922 (1976)

[2] G. P. Kushto, P. F. Souter, L. Andrews, J. Chem. Phys. **108**, 71-21-7130 (1998)

[3] A. A. Granovsky, J. Chem. Phys. **134**, 214113-1-214113-14 (2011)

[4] http://www.nist.gov/

Spectroscopic studies of bismuth containing electrodeless light sources working in self-modulating regime.

Annija Fridmane[1], Madara Zinge[1], Zanda Gavare[1,2]

[1]*Institute of Atomic Physics and Spectroscopy, University of Latvia, Skunu str. 4, Riga, Latvia, LV-1050*

[2]*Faculty of Information Technologies, Latvia University of Agriculture, Liela str. 2, Jelgava, Latvia, LV-3001*

E-mail: annijafridmane@gmail.com

High frequency electrodeless lamps (HFEDLs) are used as light sources in atom absorption spectrometers and it is of high importance to ensure that these light sources are stable and long lasting emitters of the necessary spectra. But sometimes, at higher voltage values of excitation generator, a self-modulation regime can be observed - the intensity of emission from the lamp changes periodically.

In this work we study changes of spectral line intensities during the self-modulation regime of high frequency electrodeless lamps containing bismuth as element of interest and argon as buffer gas. More precisely, there are two different fillings for the lamps under study: (1) BiI_3 + Ar (buffer gas pressure 3.1 Torr) and (2) Bi + SbI_3 + Ar (buffer gas pressure 2.8 Torr). The spherical vessel of the lamp is made of SiO_2, 1 cm in diameter. For the excitation of plasma the lamp is placed in electromagnetic field with frequency 250 MHz. The emission spectra of the HFEDLs were registered using JobinYvon SPEX 1000M high resolution spectrometer (grating 1200 lines/mm, focal length 1 m) with charge-coupled device matrix detector (2048x512 Thermoelectric Front Illuminated UV Sensitive CCD Detector, Simphony). The working conditions were chosen so that the HFEDLs work in self-modulation regime.

The intensity changes during the self-modulation regime for several elements (Bi, Ar, I, Sb) will be shown graphically in dependence on the voltage of excitation generator. It is observed that the self-modulation period becomes shorter as the voltage of excitation generator is increased.

Single shotfiber dispersion characterization with white light interferometry

Sandhra-Mirella Valdma[1], Heli Lukner[1]

[1]*Institute of Physics, University of Tartu, W. Ostwald st. 1, Tartu 50411, Estonia*

*E-mail: sandhra-mirella.valdma@ut.ee,

During the recent years the optical fiber industry has seen a considerable growth [1]. This in turn has increased the development of new types of fibers, which has established a need for convenient and quick dispersion measurement technique over a wide spectral range.

Among various methods for measuring dispersion in optical fibers [2] - spectral interferometry (SI) is the most widespread arrangement. It involves scanning delay between two consequent pulses and registering intensity or modulation pattern in the spectral domain [3]. Spatial-spectral interferometry (SSI), where the delay is mapped to the axis perpendicular to the spectral one, allows to retrieve spectral phase, group delay, and dispersion from a single trace without scanning, and is estimated to be most precise method to characterize dispersion [4].

In this work we used a customized fiber fed SSI arrangement, called SEA TADPOLE [5] for characterizing chromatic dispersion of single-mode fibers. To enhance the bandwidth we balance the dispersion of the fiber by placing known dispersion to the reference arm. That would yield a single shot measurement with a spectral phase for all the measured wavelengths [6].

In this paper we present the design based on SEA TADPOLE and demonstrate proof of principle experiments. In combination with spatially coherent supercontinuum laser source (Fianium WL-SC400-4-PP), and silicon CMOS matrix detector we can perform dispersion measurement from 400 to 1000 nm. We characterize the dispersion of single mode fiber Thorlabs 630HP in its single-mode regime 630-770 nm and compare it with dispersion curve provided by the manufacturer.

With elaborated dispersion balancing the spectral sensitivity range can be extended and potentially modes in multi-mode regime separated. Also, it is possible to extend the working range of SEA TADPOLE interferometer to telecom range with appropriate matrix sensor or suitable filtering. All in all we find that this method has high potential for commercialization.

References

[1] http://www.grandviewresearch.com/industry-analysis/fiber-optics-market

[2] L. Cohen, J. of Lightwave tech., vol. 3, p. 958 - 966 (1985)

[3] C. Froehly, A. Lacourt and J.C. Vienot, Nouvelle Revue D'Optique, vol. 4, p.183. (1973)

[4] A. Brzsnyi, A. P. Kovcs, M. Grbe, and K. Osvay, Opt. Commun. vol. 281, p. 30513061 (2008)

[5] P. Bowlan, P. Gabolde, A. Shreenath, K. McGresham, R. Trebino, and S. Akturk, Opt. Express, vol. 14, p. 11892-11900 (2006)

[6] P. Piksarv, A. Valdmann, H. Valtna-Lukner, R. Matt, and P. Saari, Opt. Lett. vol. 38, p. 1143-1145 (2013)

Measurement of ODMR signals from NV centers in diamond crystal, analysis of the signals

Mārcis Auziņš[1], Andris Bērziņš[1], Laima Bušaite[1], Ruvins Ferbers[1], Florians Gahbauers[1], <u>Reinis Lazda</u>[1,*]

[1] *University of Latvia, Faculty of Physics and mathematics, Laser Centre, Zeļļu street 8, Riga, Latvia, LV-1002*

[*]*E-mail:* reinis.lazda@lu.lv

In this work the optically detected magnetic resonance method [1] is used to study the hyperfine level structure of NV centers in diamond crystal (color defects consisting of one carbon atom substituting nitrogen atom N and a vacancy V pair). Figure 1 shows how the contrast of the measured ODRM signals changes depending on the aplied external magnetic field along the axis of the NV centers (one of the four possible directions in the diamond crystal).
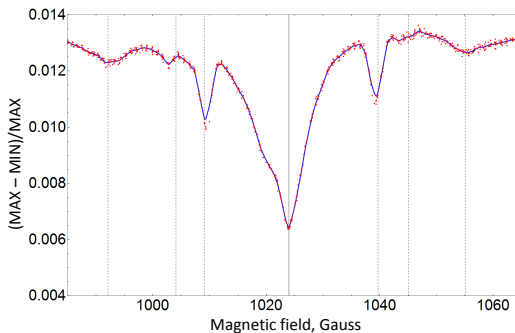

Figure 1: Contrast (calculated, maximum value of the ODMR signal minus the minimum value divided by the maximum value) of the measured ODMR signals at different magnetic field values around the GSLAC point, vertical solid black line.

The vertical dotted lines in figure 1 show the magnetic field values at which cross relaxation [2] with other defects in the diamond crystal (P1 centers here) takes place, these positions (magnetic field values) can be calculated using the Hamiltonian method.

Acknowledgements

References

[1] M. Negyedi, J. Palots, B. Gyre, S. Dzsaber, S. Kollarics, P. Rohringer, T. Pichler, and F. Simon, Review of Scientific Instruments **88**, 013902 (2017)

[2] Seiji Armstrong et al., Physics Procedia **3**, 15691575 (2010)

Laser physics and spectroscopy: posters

Spectral comparison of As and Hg containing high frequency electrodeless lamps and hollow cathode lamps

Anda Abola[1,*]

[1]*Institute of Atomic Physics and Spectroscopy, University of Latvia, Skunu Str 4, Riga, Latvia, LV-1050*

[*]*E-mail:* anda.aabola@gmail.com

When thinking about atomic absorption spectrometry, there are several kinds of light sources available, that can be used for analysis. In this work I compare arsenic and mercury containing light sources of two kinds - high frequency electrodeless lamps (HFEDLs) and hollow cathode lamps (HCLs).

To obtain spectra for analysis three types of lamps with arsenic as the main element of interest are used - (1) commercially available HCL with As+Ne filling, (2) commercially available HFEDL with As+Ar filling and (3) selected group of HFEDLs made in our institute (also As+Ar filling). For mercury there are spectra of two light sources analyzed - (1) commercially available HCL with Hg+Ne filling and (2) commercially available HFEDL with Hg+As filling.

Lamps are operated at different excitation generator voltage values, depending on their characteristics (geometry, filling), with specific attention on optimal working conditions for commercially available light sources. The emission spectra are registered using spectrometer Jobin Yvon SPEX 1000M.

Results show that when operated at optimal excitation generator voltage and current values, HFEDLs have more intense spectral lines than HCLs for both, mercury and arsenic. Differences in spectra of HFEDLs are small and are mainly based on making process and aim of usage, as, for example, some lamps made in institute have impurities, resulting in observation of molecule spectrum.

Spectral investigation of thallium containing high frequency electrodeless lamps

Arvis Gabranovs[1,*], Anda Abola[1], Madara Zinge[1]

[1]*Institute of Atomic Physics and Spectroscopy, University of Latvia, Skunu Str 4, Riga, Latvia, LV-1050*

[*]*E-mail:* arvis.gabranovs@gmail.com

Because of their geometry and spectral characteristics, high frequency electrodeless lamps (HFEDLs) are used for various applications, including atomic absorption spectrometry and plasma studies. In this work we compare emission spectra of several thallium containing HFEDLs made at Institute of Atomic Physics and Spectroscopy.

HFEDLs are made of SiO_2 glass, and are filled with buffer gas (here - argon) and working element, in this case - thallium. Lamps are spherical, with diameter of 10mm. They have a short sidearm. For investigation we used HFEDLs with slightly different fillings - Tl^{205}+SbI_3+Ar, Tl^{205}I+Ar, Tl+ TlI+Ar.

To excite the plasma the lamp is placed in an electromagnetic field with frequency of 250 MHz. Then lamps are operated at different excitation generator voltage values (21 - 29 V). The emission spectra of the light sources are registered using spectrometer Jobin Yvon SPEX 1000M.

The preliminary results show that iodine in the HFEDLs influence their operational stability and intensity of spectral lines. Also there is some mercury spectrum observed. As expected in general there is increase in intensity of thallium spectral lines, when excitation generator voltage is increased.

TESTING OF THE EXCITED VIBRATIONAL AND ROTATIONAL STATES CALCULATION ACCURACY PERFORMED BY THE DVR METHOD

A.A. Kravchenko[*], A.E. Malevich, E.Z. Shalamberidze, G.A. Pitsevich

Physiscs Department, Belarusian State University, Nezavisimosti Ave. 4, Minsk, Belarus, 220030

[*]*E-mail:* vicious001@mail.ru

Discrete Variable Representation (DVR) method is a powerful tool for numerical solving of quantum mechanics differential equations. This method was first represented by Harris et al. [1]. While the Fourier and many other methods for solving differential equations which are based on expansion of both the wave function and the potential energy over a basis set of orthogonal functions require coefficients of these functions to be found, in the case of DVR method its sufficient to know potential energy values at the nodes of a regular grid. Recently we compared possibilities of DVR and Fourier methods for determining energies of stationary vibrational states in the case of smooth and discontinuous potential energy surfaces [2] and the advantage of the first method was shown. However most of the Schroedinger equations considered had constant coefficients and didnt have analytical solutions. In order to estimate the accuracy of stationary states energy calculations by the DVR method, we used Schroedinger equation for a rotator with a free axis (1), which has an analytical solution.

$$-Fctg\Theta\frac{\partial\Psi}{\partial\Theta} - F\frac{\partial^2\Psi}{\partial\Theta^2} - F\frac{1}{sin^2\Theta}\frac{\partial^2\Psi}{\partial\phi^2} = E\Psi \tag{1}$$

In accordance with the analytical solution, the energy of the system is determined by the expression $E_l=Fl(l+1)$, where $l=0,1,2,3...$ The value of F is equal to 15 cm^{-1}. Hamiltonian matrix was built by calculating matrix elements in nodes of the 2D uniform grid. Coordinates of the grid varied in the following ranges: $0 \leq \Theta \leq \pi$; $0 \leq \phi \leq 2\pi$. As a result of diagonalization of the Hamiltonian matrix the following values were obtained for several most deeply located energy levels: 0, 30, 30, 30, 90, 90, 90, 90, 90 cm^{-1}. If we recall that energy levels of a rotator with a free axis are *2l+1* times degenerate, then it becomes obvious that the DVR method demonstrates the remarkable accuracy of the calculations.

References

[1] D. Harris, G. Engerholm, W. Gwinn, J. Chem. Phys. **43**, 1515 (1965)
[2] G. Pitsevich, A. Malevich, J.Appl.Spectrosc. **82**, 893 (2016)

Fourier-transform spectroscopic study and deperturbation analysis of the A~b complex in Cs$_2$ molecule by laser induced fluorescence

V. Krumins[1,*], A. Znotins[1], A. Kruzins[1], I. Klincare[1], M. Tamanis[1], R. Ferber[1], E.A. Pazyuk[2] and A.V. Stolyarov[2]

[1] *Laser Centre, University of Latvia, Rainis blvd. 19, Riga, Latvia, LV-1586*

[2] *Department of Chemistry, Lomonosov Moscow State University, 119991 Moscow, Leninskie gory 1/3, Russia*

[*] *E-mail:* valtskr@inbox.lv,

One of the defining characteristic properties of diatomic alkali homonuclear and heteronuclear molecules are their strongly coupled lowest excited states A$^1\Sigma^+$and b$^3\Pi$. This is because of the strong spin-orbital interaction between the mentioned states. Therefore A$^1\Sigma^+$and b$^3\Pi$ states may be considered as a single A~b complex with complicated energy level structure.

The study of A~b complex is relevant because it can be used as an intermediate state for transfer of vibrationally excited cooled molecules into their absolute rovibronic ground state X$^1\Sigma^+$(v$_x$=0, J$_x$=0). Detailed experimental study and coupled-channel deperturbation analysis is necessary in order to provide an accurate description of the A~b complex.

Present work is continuation of the study [1] in which the A$^1\Sigma_u^+$ and b$^3\Pi_u$ states of Cs$_2$ molecule were examined. The purpose of this work is to obtain more systematic data in larger energy range and to apply coupled - channel deperturbation analysis in order to describe the A~b complex with an experimental accuracy of 0.01 cm^{-1}.

Cesium molecules were produced in a stainless steel heat-pipe. The titanium-sapphire laser (MBR 110, Coherent) and various diode lasers were used for excitation. Fourier transform spectrometer (Bruker IFS125 HR) was used to register laser induced fluorescence spectra A~b $\to$ X$^1\Sigma^+$ with a resolution of 0.03 cm^{-1}. Applying direct excitation of the A~b complex nearly 4000 term values have been obtained and involved it the fit. The refined deperturbation model can reproduce the majority of term values (more than 95%) of the A~b complex with a very small standard deviation of 0.005 cm^{-1}.

References

[1] Jianmei Bai et. al., Phys. Rev. A **83**, 032514 (2011).

Banknote forgery detection at triple-wavelength illumination

Peteris Potapovs, Ilze Osina, Janis Spigulis *Biophotonics Laboratory, Institute of Atomic Physics and Spectroscopy, University of Latvia, 19 Rainis Blvd., Latvia, Riga, LV-1586 E-mail:* peteris.potapovs@lu.lv,

Counterfeit banknotes become less detectable by sensors and detection methods used in automatic teller machines (ATM). The cause is that lowering costs of scanning, printing and manufacturing technologies have led to the improvements in banknote forgery techniques. Banks are interested in a fast method for determination of counterfeit banknotes and their forgery technique. Fast and reliable technique would allow to save money and time by letting expertise institutions to choose a proper further inspection method of counterfeit banknotes.

Main objective is to create a fast and relatively cheap technique (picture processing program) which would decrease the percentage of undetected counterfeit banknotes and be able to identify a forgery technique.

The technique is developed by illuminating banknotes with three different wavelength lasers (448nm, 532nm and 659nm) simultaneously, taking pictures with RGB camera, processing pictures on a computer program and researching differences in light absorption of laser light between real and counterfeit banknotes. **References**

[1] J.Spigulis, L.Elste. "Single-snapshot RGB multispectral imaging at fixed wavelengths: proof of concept." Proc.SPIE, 8937, 89370L (2014).
[2] D.Jakovels, J.Spigulis, "2-D mapping of skin chromophores in the spectral range 500-700 nm", J.Biophoton. 3, 125-129 (2010).
[3] I.Kuzmina, I.Diebele, D.Jakovels, J.Spigulis, L.Valeine, J. Kapostins, A. Berzina, "Towards noncontact skin melanoma selection by multispectral imaging analysis", J. Biomed. Opt. 16, 060502 (2011).

On spatial resolution of optical fiber as high resolution probe

Valle Morel[1], Sandhra-Mirella Valdma[1], Heli Valtna-Lukner[1,*]

[1] *Institute of Physics, Univeristy of Tartu, W. Ostwaldi 1, Tartu, Estonia, 50411*

[*] *E-mail:* heli.lukner@ut.ee,

On several occasions optical fibers are used as a probe in order to sample or to scan spatial distribution of optical field [1]. Often the mode field diameter of the fiber is used to indicate the spatial resolution of the fiber, but this approach is not fully accurate. In presented research we study the spatial resolution of single-mode step index fibers and endlessly single mode photonic crystal fibers [2]. Theoretical framework and numerical simulations to explain experimental results are presented.

It appears, that in case of 2-dimensional bipolar transverse structures of the incident field, the features smaller than the width of the fiber mode field diameter can be detected. In order to study the spatial resolution of fiber-probe, we design and generate well described optical field pattern(s) with numerical aperture higher than that of the fiber, sample the field with the fiber, and detect the relative intensity at the fiber output. We use diffraction limited focal spot of high numerical aperture all-reflective Schwarzschild microscope objective and focused Bessel beam [3] as the test-fields. The Bessel fields are of special interest because they are eigenfunctions to 2-dimensional convolution integral with Gaussian field and hence the convolution integral follows closely the shape of the Bessel field even if the peak of the latter is narrower than the width of the Gaussian. The fields are sampled to single-mode step index fiber 630HP (Thorlabs) and endlessly single mode photonic crystal fiber (ESM PCF) LMA-5 (NKT Photonics). See Fig. 1.
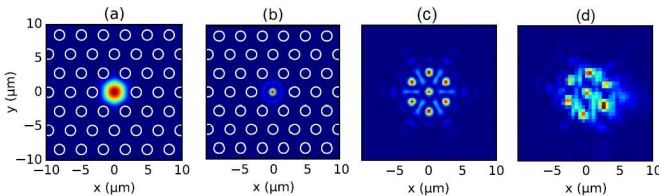

Figure 1: Numerically simulated mode field profile of ESM PCF (a), focal field of Schwarzschild objective (b), simulated coupling integral for intensity (c) and detected field (d).

At the cost of lost intensity we were able to detect the features of the incident field 1.6 to 2.5 times smaller than the corresponding width of the fibers mode field diameter for SIF and ESM PCF respectively. Also, formation of peculiar intensity patterns, arising from hexagonal low-intensity distribution of fiber mode were observed and explained.

References

[1] P. Bowlan, P. Gabolde, M. A. Coughlan, R. Trebino, and R. J. Levis, J. Opt. Soc. Am. B **25**, A81A92 (2008).

[2] Heli Valtna-Lukner, Jaagup Repän, Sandhra-Mirella Valdma, and Peeter Piksarv, Appl. Opt. **55**, 9407-9411 (2016).

[3] Heli Valtna-Lukner, Pamela Bowlan, Madis Lõhmus, Peeter Piksarv, Rick Trebino,

THE INFLUENCE OF THE DISPERSION INTERACTION ON STRUCTURAL AND SPECTROSCOPIC PROPERTIES OF THE PROTONATED WATER DIMER OBTAINED BY COMPARING RESULTS OF THE CALCULATIONS AT B3LYP/acc-pVTZ AND B3LYP-D3/acc-pVTZ LEVELS OF THEORY

A.S. Vasilevich[*], E.Z. Shalamberidze, G.A. Pitsevich

Physiscs Department, Belarusian State University, Nezavisimosti Ave. 4, Minsk, Belarus, 220030

[*]*E-mail:* godcratos1@mail.ru

Protonated water dimer (PWD) plays an important role in proton transfer processes occurring in liquid and gaseous water phases. PWD is the subject of numerous studies carrying out with the use of both theoretical and experimental methods. It was found that PWD can exist in equilibrium (with C_2 symmetry) and transition (with C_S symmetry) configurations having very close internal energies. However, by the present time there have been no any investigations of the dispersion interaction effect on spectral and structural parameters of the equilibrium and transition form of the PWD. To analyze this situation calculations of the geometry parameters as well as IR spectra in harmonic and anharmonic approximation were made using B3LYP/acc-pVTZ and B3LYP-D3/acc-pVTZ levels of theory. The results of the calculations are presented in Table 1.

Table 1: Some geometry parameters of the PWD obtained during optimization at B3LYP/acc-pVTZ and B3LYP-D3/acc-pVTZ levels of theory.

Level of theory	l_{O--O} [Å]	l_{O-H} [Å]	δ_{O-H-O} [deg]	$\tau_{H-O-O-H}$ [deg]
C_2 configuration				
B3LYP/acc-pVTZ	2.40295	1.20299	174.24	40.91
B3LYP-D3/acc-pVTZ	2.40230	1.20275	174.10	39.12
C_s configuration				
B3LYP/acc-pVTZ	2.40047	1.16001	1.24219	111.67
B3LYP-D3/acc-pVTZ	2.39986	1.15856	1.24278	111.87

As one can see from Table 1 dispersion interaction makes H-bond little bit more strong in both PWD configurations. According to calculations taking into account the dispersion interaction leads to lowering the internal energy by 280 cm^{-1} in both configurations. The influence of the dispersion interaction on spectral parameters of the PWD is more pronounce. For example the anharmonic frequency of the most interesting stretching shared proton vibration rising by 20 cm^{-1} in equilibrium configuration of the PWD if dispersion interaction is taken into account. Few additional sensitive to dispersion interaction vibrational modes were also found in both configuration.

3D PES ASSOCIATED WITH DONOR HYDROXYL GROUP MOTIONS IN WATER DIMER. STRETCHING AND BENDING OH VIBRATIONS STUDIED AT MP4/acc-pVTZ LEVEL OF THEORY

A.U. Vasilevski*, E.Z. Shalamberidze, N. Tsimbrovsky,
A.E. Malevich, E.N. Kozlovskaya, G.A. Pitsevich

Physiscs Department, Belarusian State University, Nezavisimosti Ave. 4, Minsk, Belarus, 220030

E-mail: sasha.vasilevski20@gmail.com

Water dimer (WD) is the simplest water cluster that plays an important role in chemical reactions occurring in the Earth atmosphere. Thus studying of this cluster has theoretical and practical aspects. Taking into account the anharmonicity of the donor O-Y group vibrations in WD one has to know multidimensional potential energy surface (PES) for large amplitude motion of the donor hydrogen atom. First of all, the equilibrium geometry of the WD was found at MP4/acc-pVTZ level of theory. Then the origin of the Cartesian coordinate system was placed at the donor hydrogen atom, X axis was directed along O-H bond, Y axis was located in the plane formed by atoms of the hydrogen bridge, and Z axis supplemented axes X and Y to the right-hand triple. Then the donor H atom was moved along X, Y and Z axis with 0.1 Å step while coordinates of all other atoms were fixed. 3D PES was calculated in all nodes of the 3D net in a parallelepiped with the sides $-0.4 \leq X \leq 0.8, -0.7 \leq Y \leq 0.7, 0 \leq Z \leq 0.7$. To find frequencies of the donor hydroxyl group vibrations the following Schroedinger equation was solved using DVR method:

$$-\frac{\hbar^2}{2\mu_{OH}}\frac{\partial^2\Psi}{\partial x^2} - \frac{\hbar^2}{2\mu_{OH}}\frac{\partial^2\Psi}{\partial y^2} - \frac{\hbar^2}{2\mu_{OH}}\frac{\partial^2\Psi}{\partial z^2} + U(x,y,z)\Psi = E\Psi \qquad (1)$$

where $\mu_{OH} = \frac{M_0 M_H}{M_0 + M_H}$ is the reduce mass of the H and O atoms; $x = \frac{X}{l_0}$; $y = \frac{Y}{l_0}$; $z = \frac{Z}{l_0}$; $l_0 = 1$Å.

As the result of these calculations frequencies of all fundamental as well as overtones and combination vibrations of the donor hydroxyl group were found in 0-4200 cm^{-1} energy range. The calculated fundamental frequencies of out of plane and in plane bending vibrations are equal to 534 and 1230 cm^{-1} respectively while the frequency of the stretching vibration is equal to 3568 cm^{-1} and its in a good agreement with experimental value (3575 cm^{-1}).

Spectroscopic study of the $(4)^1\Pi$ state of RbCs molecule by laser induced fluorescence

<u>A. Znotins</u>[1], A. Kruzins[1], I. Klincare[1], M. Tamanis[1], R. Ferber[1], E.A. Pazyuk[2] and A.V. Stolyarov[2]

[1]*Laser Centre, University of Latvia, Rainis blvd. 19, Riga, Latvia, LV-1586*

[2] *Department of Chemistry, Lomonosov Moscow State University, 119991 Moscow, Leninskie gory 1/3, Russia*

*E-mail:*znotins.aigars@gmail.com,

Observation and analysis of laser induced fluorescence (LIF) spectra of $A^1\Sigma^+$ and $b^3\Pi$ states ($A-b$ complex for short) from $(3)^1\Pi, (4)^1\Sigma^+$ and $(5)^1\Sigma^+$ states in RbCs was reported [1]. It was shown that high accuracy description of the $A-b$ complex based on coupled-channel deperturbation treatment achieved in [1], allows the use of $A-b$ complex as an intermediate state in order to reach higher electronic states in RbCs by two – step excitation process. This work is devoted to the study of $(4)^1\Pi$ state by applying two – step excitation and observation of the $\neg$ $(4)^1\Pi \to$ $X^1\Sigma^+$ LIF . This state was first observed and described in [2]. The aim of the present work was to obtain systematic term value data for the rovibronic levels and to construct the potential energy curve. In the experiment RbCs molecules were produced in a linear heat pipe at 310 ^{o}C. The radiation of two Coherent MBR-110 Ti:Saphire lasers was used to excite transitions from the ground state to the $A-b$ complex and then, in second step excitation, from $A-b$ complex to $(4)^1\Pi$ state. LIF spectra were recorded by Fourier transform spectrometer (IFS 125-HR, Bruker) in the 10000-22000 cm^{-1} spectral range. Excitation frequencies for the second step were selected within the range $9800-11000$ cm^{-1} by monitoring the $(4)^1\Pi \to$ $X^1\Sigma^+$ LIF signal. The recorded spectra also contained the $A-b \to$ $X^1\Sigma^+$ transitions excited by the same laser frequencies. The assignment of the LIF progressions allowed us to determine the energy and the rotational quantum number J' of the rovibronic levels of the $(4)^1\Pi$ state. In several spectra rotational relaxation lines were observed around strong lines of the main progression, thus increasing the amount of term values and allowing to estimate λ - splitting. The obtained term values of the $(4)^1\Pi$ state were included in the single potential fit and empiricaly based point wise potential was constructed. The support from Base/Performance Funding project no. AAP2016/B013, ZD2010/AZ27 and project 1.1.1.2/VIAA/1/16/068 is gratefully acknowledged by MOLPOL team.

References

[1] A. Kruzins, *etal*, J. Chem. Phys. **141**, 184309 (2014)

[2] T. Gustavsson, *etal*, Molecular Physics **64 No 2**, 293 (1988)

OSA University of Latvia Student Chapter

SPIE. STUDENT CHAPTER
UNIVERSITY OF LATVIA

LATVIJAS UNIVERSITATE
ANNO 1919

OSA | 100
The Optical Society | Since 1916